



РОСАТОМ

КОНФЕРЕНЦИЯ «ТЯЖЕЛЫЕ ЖИДКОМЕТАЛЛИЧЕСКИЕ ТЕПЛОНОСИТЕЛИ
В ЯДЕРНЫХ ТЕХНОЛОГИЯХ»



ТОПЛИВНАЯ КОМПАНИЯ РОСАТОМА

ТВЭЛ



ВНИИМ
имени А.А.Бочвара

Mechanical properties, corrosion resistance and technological development of steel EP 823

I.A. Naumenko,

M.V. Leontyeva-Smirnova, A.A. Nikitina, M.V. Skupov

Obninsk, October 8-10. 2018

Ferritic-martensitic steel EP823

| Content of elements, wt. %. | | | | | | | | | | | | |
|-----------------------------|---------|---------|-------|--------|-------|---------|---------|---------|---------|---------|-------------|------------|
| C | Si | Mn | S | P | Cr | Ni | Mo | W | Nb | V | Ce Расч. | B Расч. |
| 0,14-0,18 | 1,0-1,3 | 0,5-0,8 | <0,01 | <0,015 | 10-12 | 0,5-0,8 | 0,6-0,9 | 0,5-0,8 | 0,2-0,4 | 0,2-0,4 | <0,1 | <0,006 |

EP823 is mastered and justified as a material for fuel pin claddings, wrapper tubes and other units of BREST-OD-300 reactor.

It was tested as a cladding of experimental fuel elements in nuclear power units with heavy metal coolant and hexagonal covers (wrappers) in BN-600.

The works are conducted in the following directions:

- Investigation and justification of corrosion resistance;
- Justification of radiation resistance;
- Technological development;
- Investigations of the structural-phase state and physic-mechanical properties at all stages of development and manufacture of product;
- Graduation of the attestation report.

Properties of metal products by grades



POCATOM

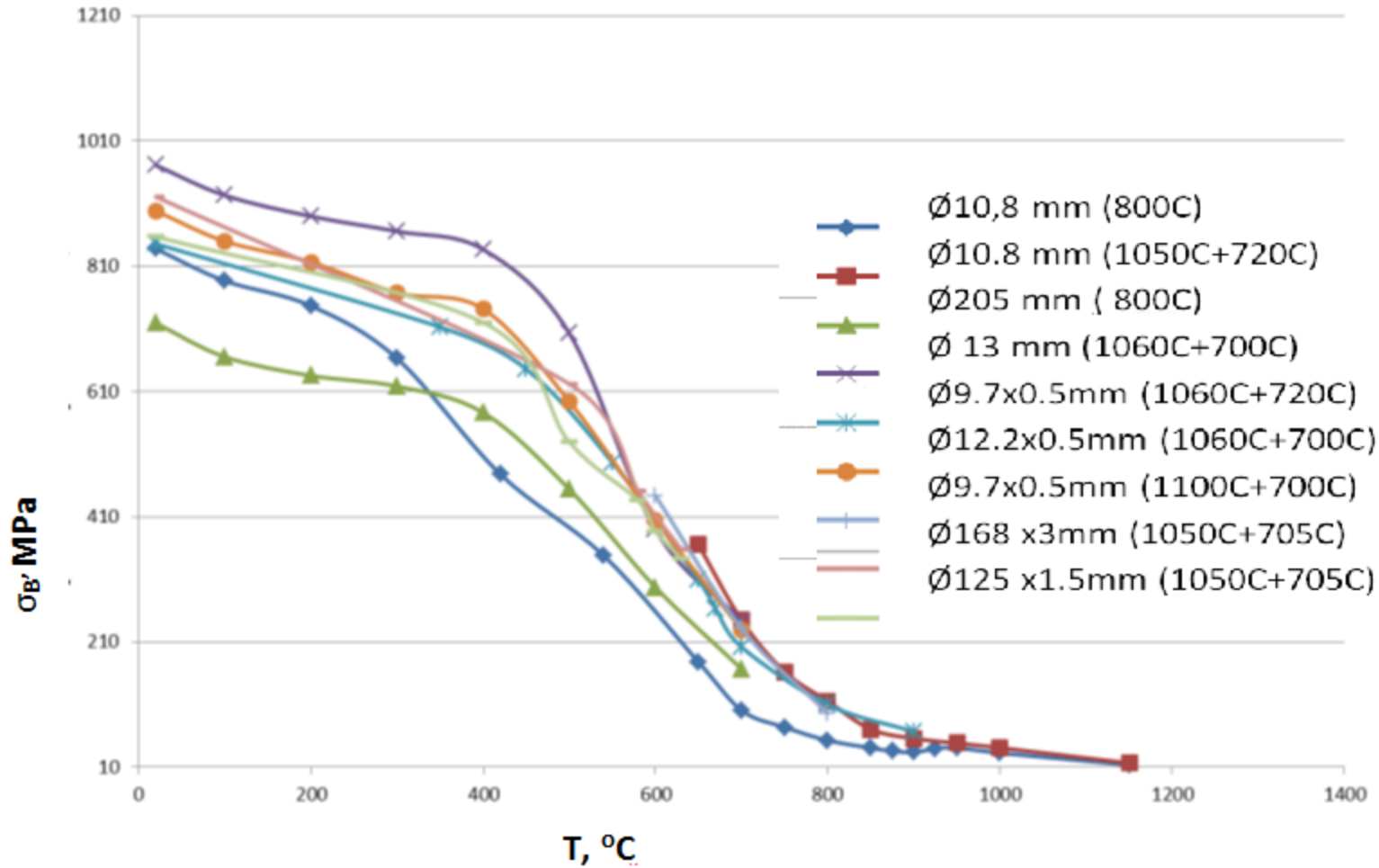
❑ **The properties of various semi-finished products from steel EP823 are obtained according to the grades:**

- **Grade 1**- Bars of various diameters and thick-walled tubes. The structure of bars $\varnothing 13\text{mm}$, $\varnothing 205\text{ mm}$, data on short-term mechanical properties (UTS, YS, elongation, constriction) in the test temperature range 20-700 °C for bars $\varnothing 13\text{mm}$, $\varnothing 205\text{ mm}$ and in the range of 20-630 °C for large diameter tubes $\varnothing 168 \times 3\text{ mm}$ and $\varnothing 125 \times 1.5\text{ mm}$, cyclic strength of samples from rod $\varnothing 205\text{ mm}$ at room temperature, long-term strength and thermal creep of samples from rod $\varnothing 205\text{ mm}$ (time to rupture at temperatures of 500-800 °C) and $\varnothing 13\text{mm}$ rod at 670 °C.
- **Grade 2** – Thin-walled tubes. The structure of tubes $\varnothing 12,2 \times 0,5\text{ mm}$, $\varnothing 9,7 \times 0,5\text{mm}$, $\varnothing 6,9 \times 0,4\text{ mm}$, data on short-term mechanical properties (UTS, YS, elongation) in the test temperature range of 20-900 °C in the initial state for samples from tubes $\varnothing 12,2 \times 0,5\text{ mm}$, $\varnothing 9,7 \times 0,5\text{mm}$.
- **Grade 3** – Hexagonal tubes and sheets, pipes with large diameter. Weldability by means of argon arc manual welding and mechanical properties of welded joints in tensile tests of 1,5 and 2,0 mm thick plates and static bending at a temperature of 20 ° C.
- **Grade 4** – Wire $\varnothing 1.05\text{ mm}$. The data on the short-term mechanical properties of the spacer wire made of steel EP823 in the temperature range of 20 - 700 ° C.
- **Grade 5** - Thin tape. The data on the short-term mechanical properties of the tape with a thickness of 0,3 mm made of steel EP823- in the temperature range 20 - 700 ° C were obtained.
- **In total, more than 35 types of metal products were produced**

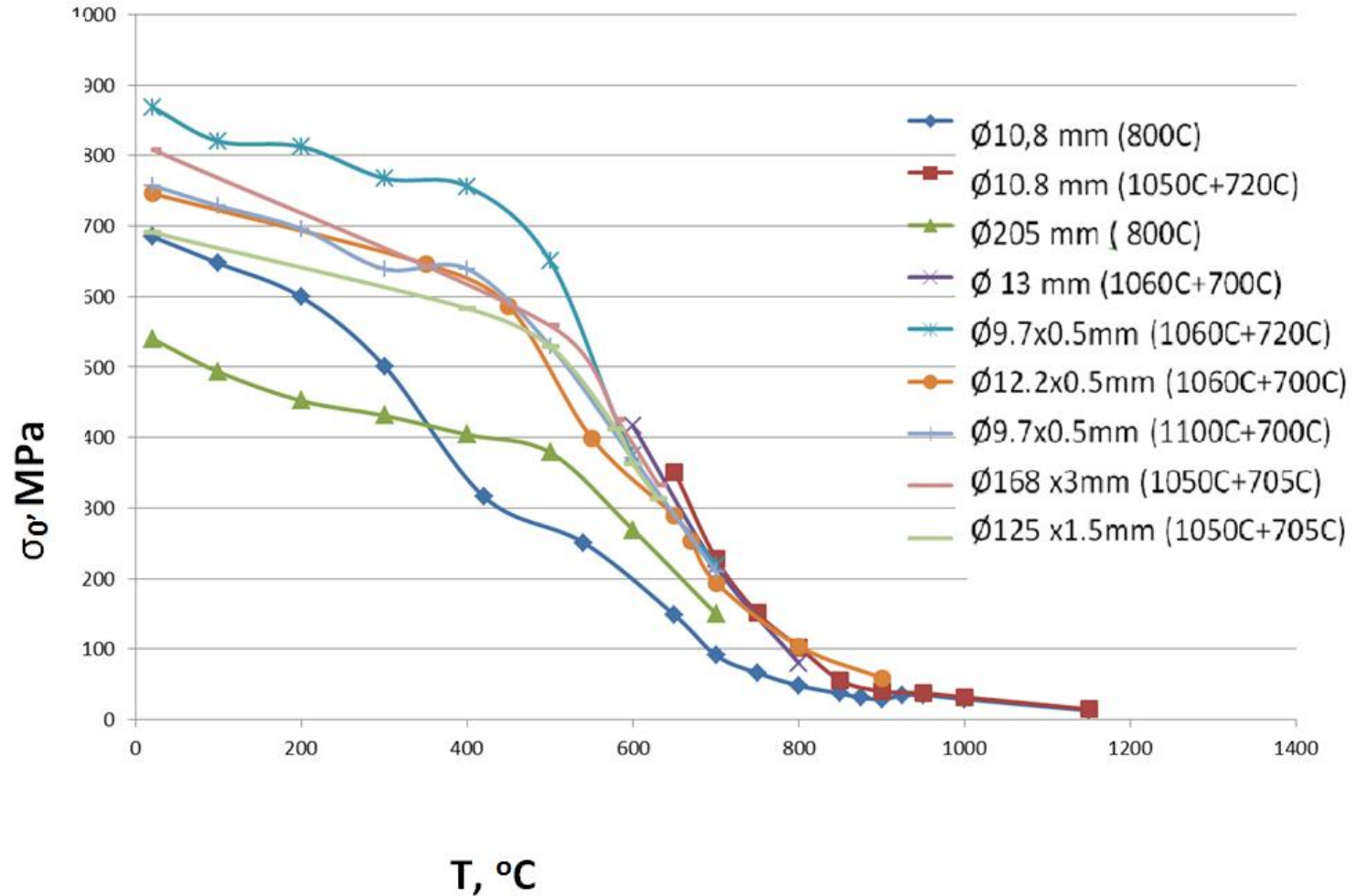
Short-term mechanical properties of various grades of EP 823 (grades 1-3)



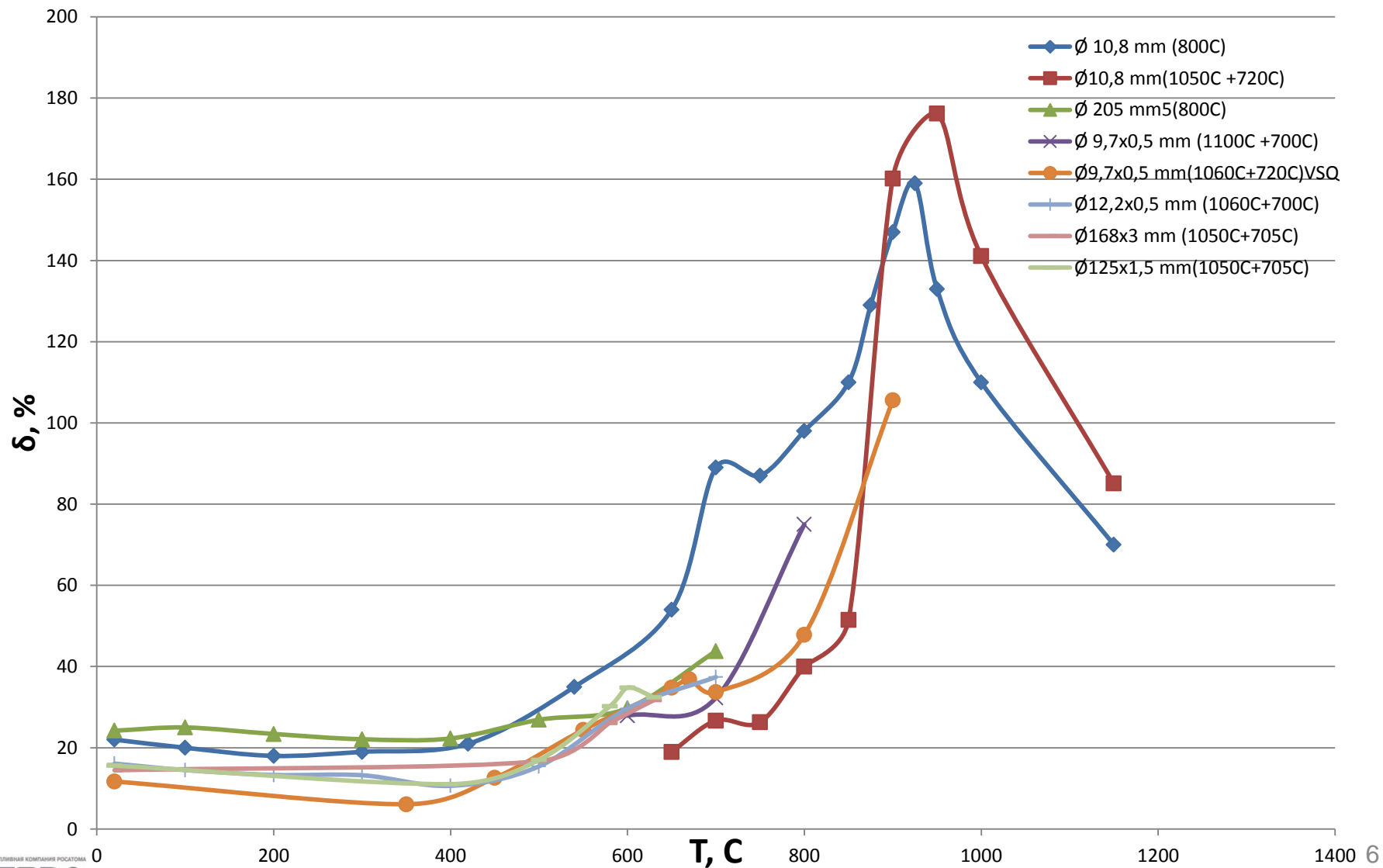
POCATOM



Short-term mechanical properties of various EP823 steel products (grades 1-3)



Short-term mechanical properties of various EP823 steel products (grades 1-3)



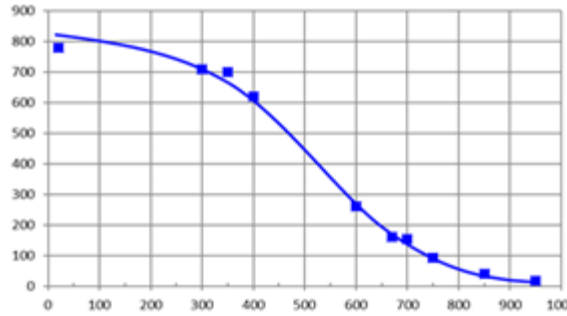
Short-term mechanical properties of spacing wire $\varnothing 1.05$ mm (grade 4)



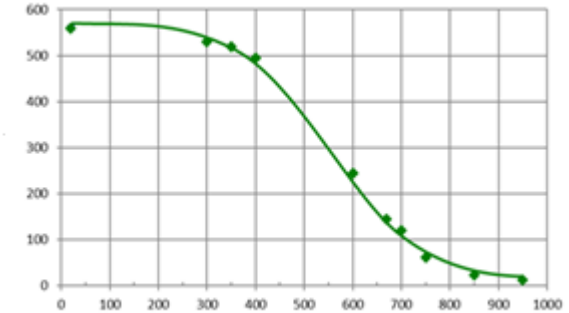
POCATOM

Tensile tests for spacing wire $\varnothing 1.05$ mm at test temperatures 20-950 ° C have been carried out.

As the test temperature increases, the strength and yield strength decreases. The elongation is maximum at 900-950 ° C



$\sigma_B, \text{MPa} - T, \text{°C}$

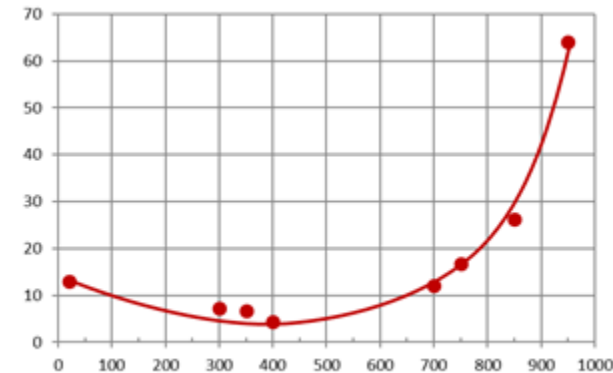


$\sigma_{0,2}, \text{MPa} - T, \text{°C}$



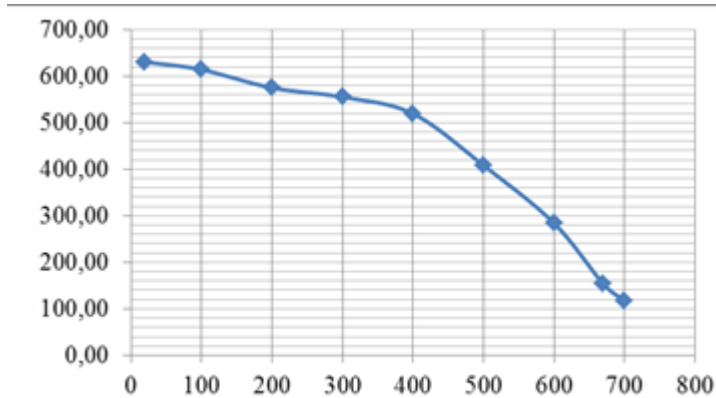
•1-liner, holding the sample; 2-hollow cylinder connecting to the rod of the test machine

The level of mechanical properties of the investigated wire requires TU 14-131-1197-2016: $\sigma_B = 790$ MPa (requirement TU 14-131-1197-2016-not less than 620 MPa); $\delta_0 = 13$ % (requirement TU 14-131-1197-2016-not less than 5 %); the number of kinks is 28-29 (requirement TU 14-131-1197-2016-not less than 10).

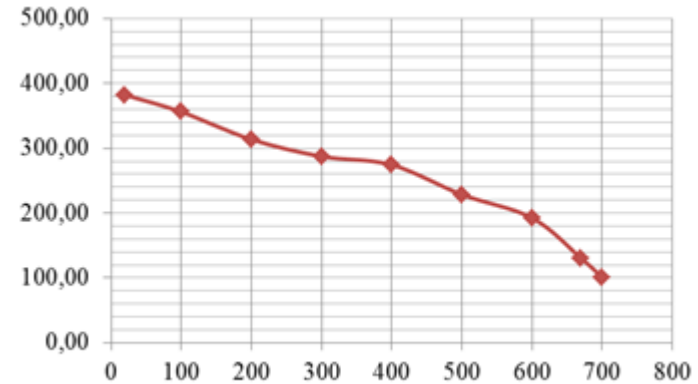


$\delta, \% - T, \text{°C}$

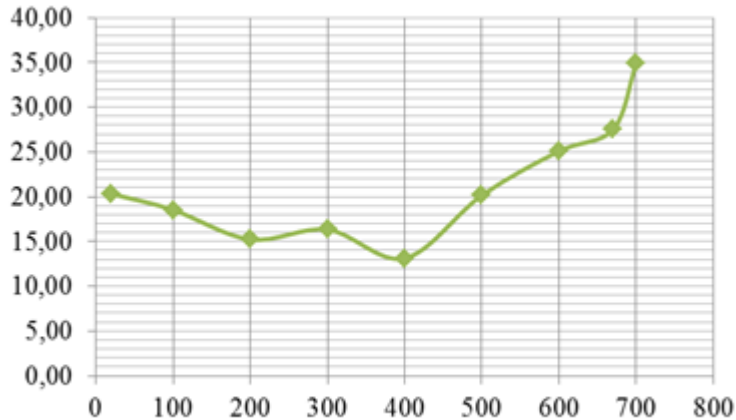
Short-term mechanical properties of flat specimens 0.3 mm thick of steel EP823 (grade 5)



σ_B,MPa - T, °C



σ_{0,2},MPa - T, °C



δ, % - T, °C

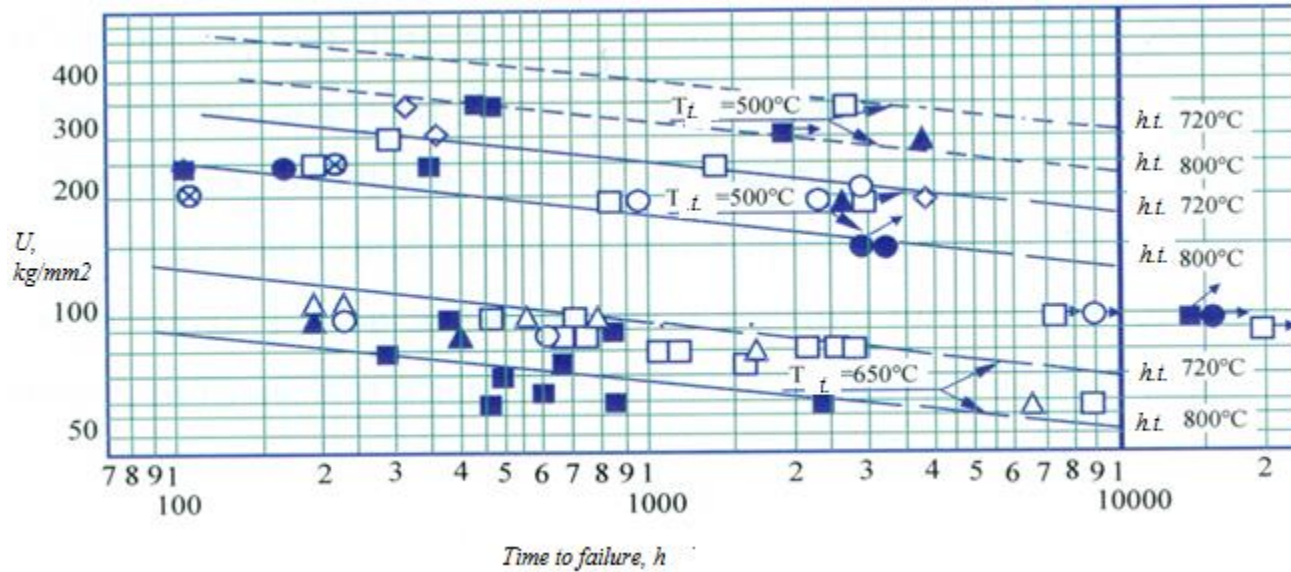
The tests were carried out to expand the technical requirements for the subsequent fabrication of the tape.

Regularities in the dependence of the strength and yield strengths - are characteristic for steel EP823.

Requirements for hardness:

HV_{0,1} ≤ 250 ± 10

Long-term mechanical properties of steel EP 823



Effect of tempering temperature on the long-term strength of steel EP823 at test temperatures 500-650 ° C

Values of the limits of the long-term strength of cladding tubes $\varnothing 9,7 \times 0,5$ mm made of steel EP823

| Test temperature, °C | σ_{3000} , MPa | σ_{10000} , MPa | σ_{20000} , MPa |
|----------------------|-----------------------|------------------------|------------------------|
| 650 | 80 | 65 | 58 |
| 670 | 51 | 41.5 | 36.5 |
| 700 | 47 | 41 | 37 |
| 750 | 15,6 | 12,3 | 10,8 |
| 800 | 10,8 | 9 | 8 |

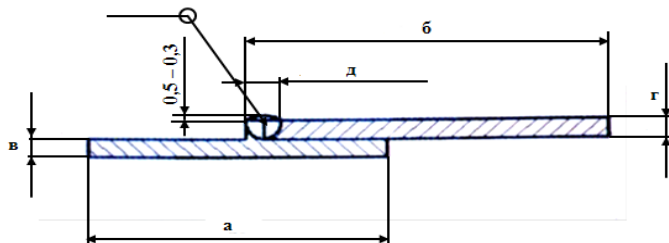
| Strength, MPa | Test temperature T , °C | Creep rate %/h | Test time, h |
|---------------|---------------------------|----------------------|--------------------------|
| 75 | 670 | $6,21 \cdot 10^{-4}$ | 4122 |
| 75 | 650 | $2,7010^{-3}$ | 546 (tests are going on) |

Properties of welded joints obtained by various welding methods applied to the EP823 steel

The list of initial metal products (technical requirements, heat treatment)

| name of metal products | technical requirements | Heat treatment, °C |
|-------------------------------|----------------------------|----------------------|
| | | quenching/ tempering |
| Sheet 2 mm cert. №501086 | 14-123-227-2011 | 1060±10/710±20 |
| Sheet 1,5 mm cert. №501086 | 14-123-227-2011 | 1060±10/710±20 |
| Sheet 5 mm cert. №2604-1 | 6300-001- 59532330-2012 | annealing 800 |

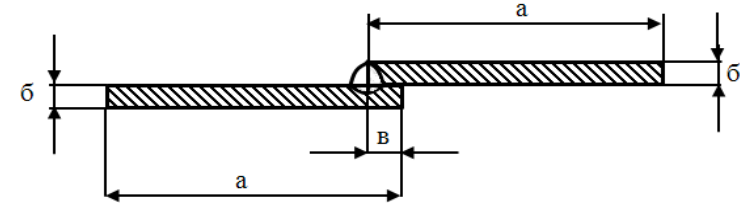
Design of joint-locking joint



variant 1: a = 100 mm; b = 100 mm; c = 2 mm; r = 2 mm ; d = (2 ± 0,5) mm;

variant 2: a = 100 mm; b = 100 mm; c = 1,5 mm; d = 1,5 mm ; e = (1,5 ± 0,5) mm

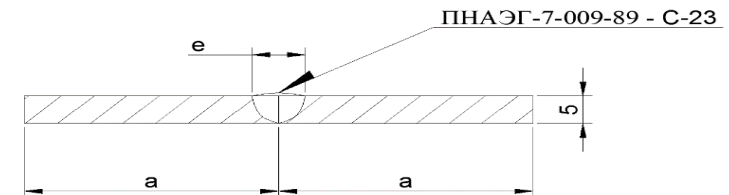
Design of a lap welded joint



variant 1: a = 50 mm; b = 1,5 mm; c = 10 mm

variant 2: a = 50 mm; b = 2 mm; c = 10 mm

Sketch weld butt welding plates



The size a is determined by the size of the semi-finished product

Welding modes are developed:

Argon arc welding regimes: for the sheet 1,5 mm current I=60 A, for 2 mm I= 80A, for 5 mm I= 120A

Laser welding regime for the samples 1,5 and 2 mm thickness: welding speed 10 s/cm, voltage 400 V,, pulse frequency 2Hz, spot diameter 1,2 mm

Properties of welded joints obtained by various welding methods, applied to the components from steel EP823

Maximum loads applied to the welded joints (argon arc welding) of the specimens before failure

| Plate thickness, mm | Type of welded joint | Test temperature, °C | Max load, kgf | |
|---------------------|----------------------|----------------------|------------------|------------|
| | | | average value | min. value |
| 1,5 | close | 20 | 1645,0 (746 MPa) | 1644,0 |
| | | 450 | 826 (561,5 MPa) | 778 |
| | | 580 | 476(323,5 MPa) | 460 |
| | | 630 | 362,5 (246 MPa) | 346 |
| | overlapping | 20 | 1325,5 | 1277,0 |
| | | 450 | 902 | 857 |
| | | 580 | 471,5 | 469 |
| | | 630 | 374 | 351 |
| 2 | close | 20 | 2203,0 (749MPa) | 2198,0 |
| | | 450 | 1147 (575 MPa) | 1127 |
| | | 580 | 732(361,5MPa) | 709 |
| | | 630 | 578,5(293,0MPa) | 575 |
| | overlapping | 20 | 1405,0 | 1383,0 |
| | | 450 | 1133 | 1133 |
| | | 580 | 718 | 684 |
| | | 630 | 452,5 | 437 |

The maximum loads applied to the welded joints of the specimens during the tension tests to failure at room temperature (argon arc welding, joint-to-joint and laser welding)

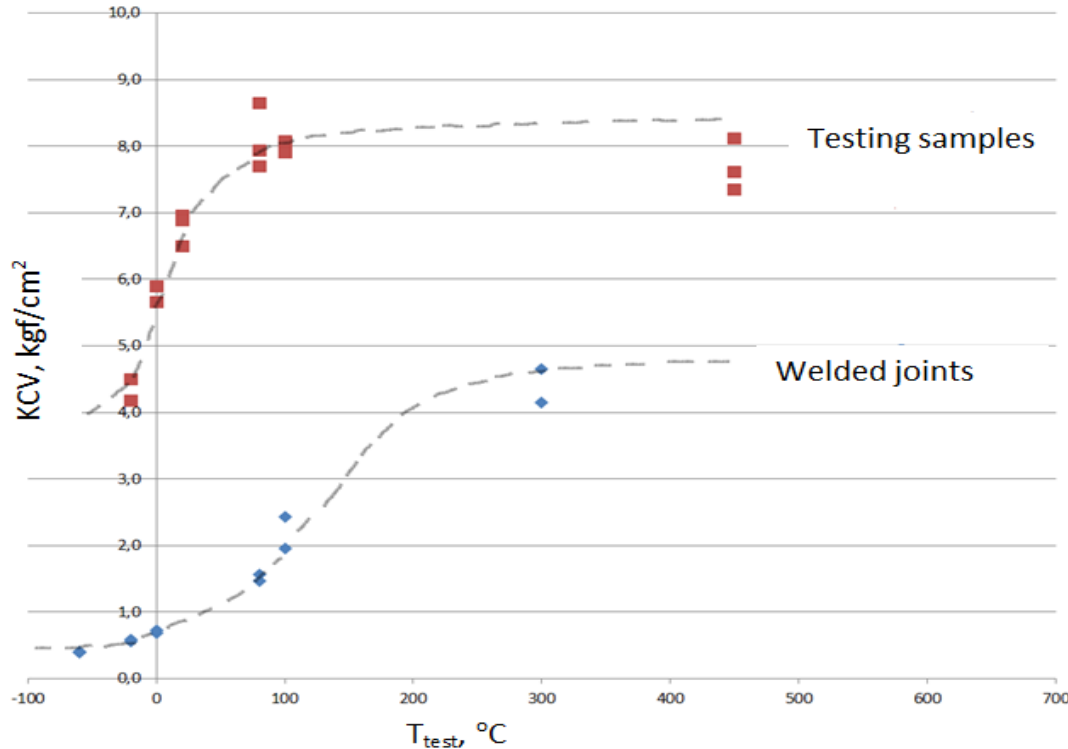
| Type of welding | Maximum load, kgf | |
|---|-------------------|--------|
| | Average | Min |
| Laser welding Sheets 1,5 mm | 1883 (640MPa) | 1565 |
| Laser welding Sheets 2 mm | 1774,5 (603MPa) | 1555 |
| Argon arc welding, joint-to-joint, sheet 1,5 mm | 1095.5 | 1056.0 |
| Argon arc welding, joint-to-joint, sheet 2,0 mm | 1271 | 1057 |

Static bending tests showed that on joint-to-joint specimens made by argon arc welding, a bending angle of more than 120 ° was obtained.

The selected welding regime makes it possible to obtain a welded joint with no brittleness at room temperature.

The maximum bending angle (before the rupture) was 80 ° on the samples made by laser welding. The probable cause is the presence of a coarse-grained structure in the weld joint, a stress concentrator.

Properties of welded joints obtained by various welding methods, applied to the components from steel EP823



The temperature of the brittle-ductile transition on samples of welded joints is 80 ° C (on the initial (before welding) samples 20 ° C)

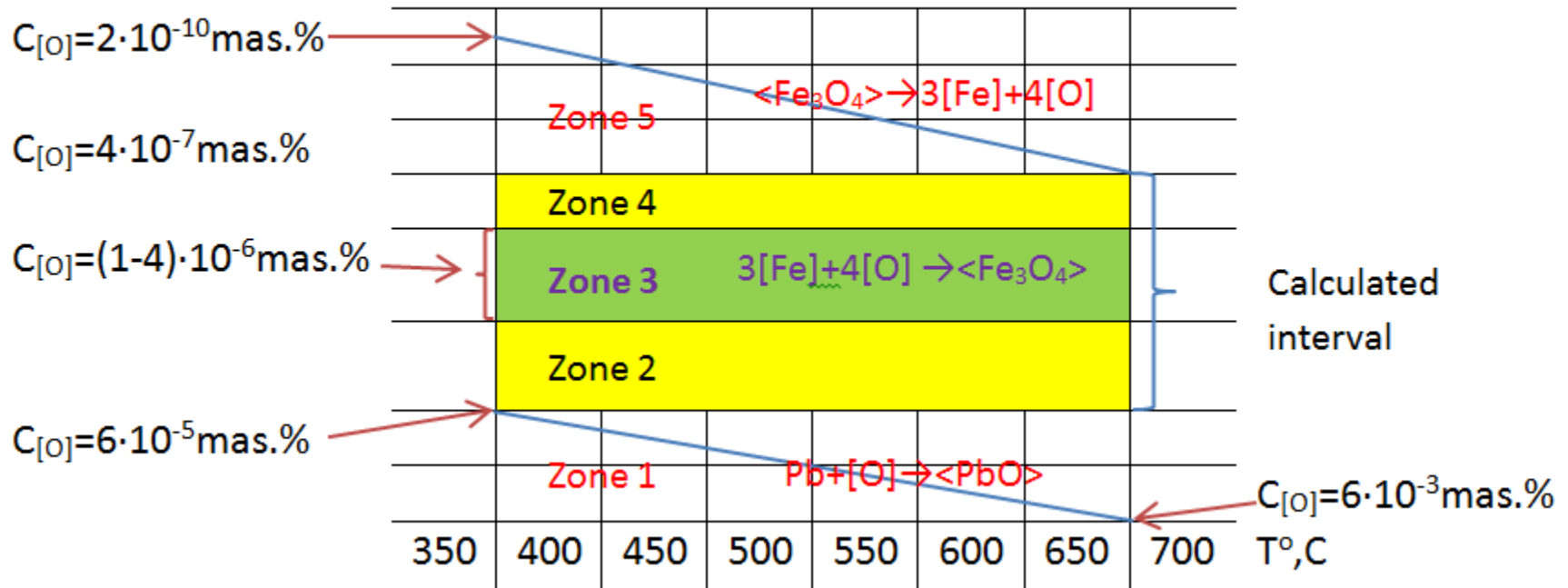
Dependence of the impact strength values, constructed from the results of testing samples of welded joints (argon arc welding, joint-to-joint) from a sheet 5 mm thickness)

Corrosion tests were carried out in a lead coolant flow in the CM-2 test bench with a concentration of dissolved oxygen $C [O] = (1-4) \cdot 10^{-6}$ wt. %, with a duration of ~ 15,000 hours at temperatures of 425 - 670 ° C. Tests of samples for corrosion resistance in lead coolant were carried out in FEI. I Express my gratitude to the staff of FEI under the leadership of Georgy Birzhevoy in testing and research of samples

Results

- ❑ No corrosion erosion damage was found on all samples.
- ❑ The thickness of the oxide film did not exceed 15 μm at each temperature (according to technical demands of BREST - no more than 50 μm).
- ❑ Liquid metal corrosion (corrosion by the dissolution mechanism) was not detected on any of the samples studied.
- ❑ The function of the protective anticorrosive barrier, which prevents the development of liquid metal corrosion of the samples in the lead coolant, is performed by the oxide layer.
- ❑ The interaction of samples with the coolant does not lead to loss of strength properties and embrittlement of the clad material.
- ❑ The mechanical properties of the samples vary within the limits typical for tube specimens subjected to normal (without irradiation) thermal aging at 650 (670) °C.
- ❑ The stability of model samples with cladding tubes made of steel EP823 to fretting corrosion at 620 ° C, ~ 5000 h, $C [O] = (1-4) \cdot 10^{-6}$ wt. %, the velocity of the coolant is ~ 1.6 m / s.

Diagram of the oxygen modes in a lead coolant of BREST-OD-300



| | |
|--------|---|
| Zone 5 | Conditions of dissolution of protective coatings. Dissolution of steel. Possibility of an emergency. Operation is unacceptable. |
| Zone 4 | Not recommended. Risks zone (no more than 1000 hours) |
| Zone 3 | Optimal interval under operation. Experimentally justified |
| Zone 2 | Not recommended. |
| Zone 1 | Conditions of PbO slagging. Possibility of an emergency. Operation is unacceptable. |

- ❑ In the BN-600 reactor, 19 experimental fuel assemblies were tested with a wrapper made of steel EP 823 in normal operation, damaging dose reached on the wrapper ~ 60 d.p.a, the maximum irradiation temperature was 600 ° C.

Exploitation conditions of the core elements of BREST-OD-300

The results of mechanical tests of the plate samples of steel EP823 after irradiation in BN-600

Fuel assembly details

T = 460-580 °C
50 – 140 dpa

Fuel pin cladding

T = 670 °C
120 – 140 dpa

T_{irrad} = 420-485 °C
55-75 dpa

T_{test} = 500 °C;
UTS = 572 MPa

T_{test} = 690 °C;
UTS = 213 MPa

T_{irrad} = 430-460 °C
86-100,3 dpa

T_{irrad} = 500 °C;
UTS = 528 MPa

Material test assembly with samples from steel EP823

- ❑ The following radiation investigations of the EP823 steel are oriented to tests in the BN-600 reactor of material test assemblies with a removable containers. The use of such containers ensures the achievement of damaging doses of 140 dpa at constant operating parameters in the temperature range 400-700 ° C.

Samples from steel EP823 (and ODS steels) for material test assemblies of для BN-600:



**Flat sample
(mechanical properties,
structure)**



**Impact sample
(impact strength,
structure)**



**Cylindrical sample
(physical properties,
structure)**



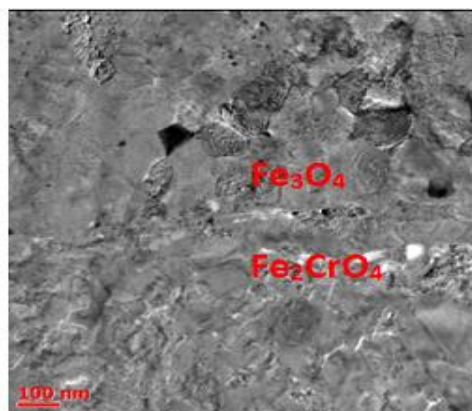
**Tube specimens under the internal
gas pressure**

Conclusion

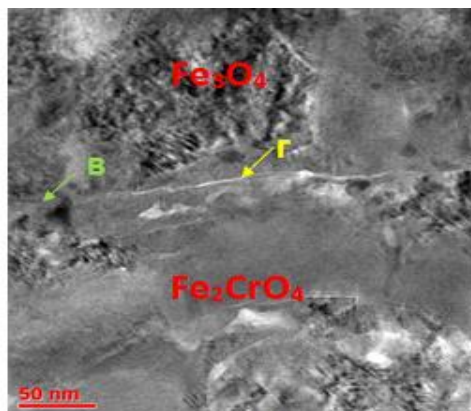


- ❑ The main thematic areas and results of works on the R&D of steel EP 823 for the core elements of the BREST-OD-300 reactor are presented.
- ❑ It is shown that on products from steel EP823 of one chemical composition, it is possible to stably obtain a complex of mechanical properties in a wide range of values that meets the technical requirements of metal products of various grades using different technologies and heat treatment regimes.

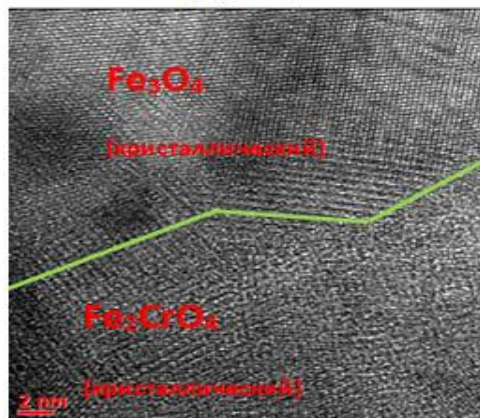
Investigation of the zone of corrosion interaction on samples of cladding tubes from steel EP823 after corrosion tests in lead at 420 °C for ~ 5000 h, oxygen content in lead-(1-4) · 10⁻⁶ wt.



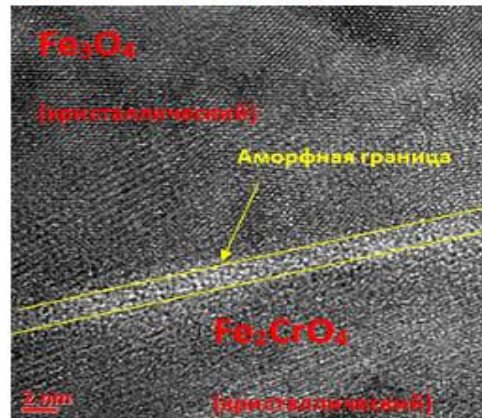
а) граница



б) общий вид



в) область 1



г) область 2

Bright-field TEM images of the oxide layer on EP823 steel after corrosion tests, boundary area between Fe₃O₄ and FeCr₂O₄

- Using high-resolution transmission electron microscopy, it has been established that the interface between magnetite and iron-chromium spinel is heterogeneous and can have both crystalline and amorphous structure. This will adversely affect the adhesion of the surface layer of magnetite to the inner oxide layer, and can lead to its detachment from the surface during operation in the circulating lead coolant.
- It has been experimentally established that the oxide layer on samples superficially doped with aluminum has a much smaller thickness (less than 100 nm), as compared to the samples of the original steel (about 3,5 μm on average over the surface). At the same time, defects, pores and discontinuities are not observed at the interface between the oxide layer and steel, which indicates the high performance characteristics of the oxide film formed during the corrosion test.

Optimization of Manufacturing Process of Functionally Graded Composite Steels for Lead-bisuth Cooled Fast reactor Cladding Application

Jeonghyeon Lee, Taeyong Kim, Il Soon Hwang, Ji Hyun Kim*

Department of Nuclear Science Engineering
School of Mechanical, Aerospace and Nuclear Engineering
Ulsan National Institute of Science and Technology (UNIST), Ulsan, Republic of Korea
*kimjh@unist.ac.kr

**2018 Heavy Liquid Metal Coolants in Nuclear Technologies (HLMC)
Obninsk, Russia Federation
2018.10.8-10**



Outlook

- 1 Introduction
- 2 Objective and Approach
- 3 Experiment & Methodology
- 4 Results and Discussions
- 5 Summary

This work was supported by the National Nuclear R&D program funded by Ministry of Science, ICT and Future Planning, and by the National Nuclear R&D program (NRF-2017M2A8A1092492) organized by the National Research Foundation (NRF) of South Korea in support of the Ministry of Science, ICT and Future Planning.

Materials for high-burnup Gen IV reactors

- Cladding materials development is a key issue to achieve high burn-up operation of Generation IV nuclear energy systems such as supercritical pressurized water reactor (SCPWR), sodium-cooled fast reactor (SFR), and lead bismuth-cooled fast reactor (LFR) and so on.
- Small Modular Reactors (SMRs) are being rapidly developed based on extensive naval experience in order to provide much higher safety and flexibility in tailoring capacity. Liquid-metal cooled fast-neutron SMRs need improved structural materials with better corrosion resistance
- The candidate cladding materials must have a high resistance to neutron irradiation embrittlement and void swelling as well as a good performance of mechanical properties at elevated temperatures.
- In addition, a **good corrosion resistance** of the claddings in the relevant environments has been certainly required for practical long term operation of those reactors.

Corrosion of F/M steels and austenitic steels

- An appropriate oxygen control in Pb or LBE are required which can determine surface oxide growth rate. **The oxide film significantly reduces corrosion.**
- With oxygen concentration above 10^{-6} wt.% in static and 10^{-6} - 10^{-5} wt.% in dynamic test condition, both austenitic and FM steels formed **protective oxide layer** under 550°C .
- Above 550°C , formation and protectiveness of oxides at austenitic steels are **unstable** and also oxides of FM steels are **thin and not completely protective.**

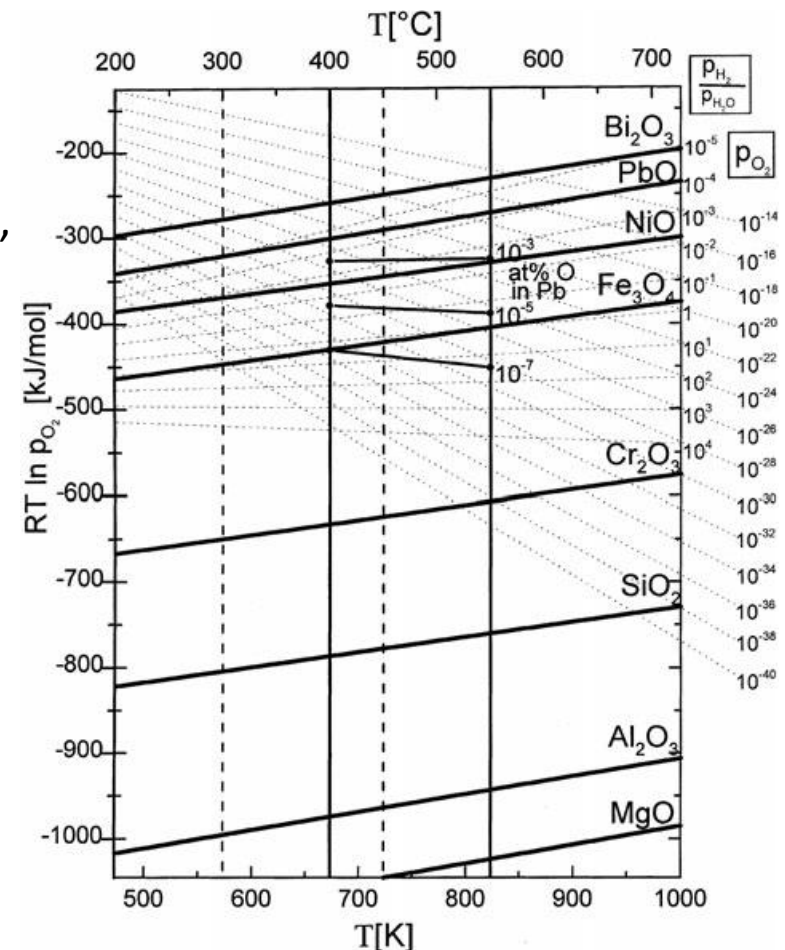


Fig. Ellingham diagram for metals and its oxides [1]

Corrosion resistant materials for LBE-FR

- SNU and KTH suggested new **Fe-Cr-Al alloy** according to corrosion test result at high temperature. [1, 2]
 - Cr and Al containing alloys shows that a thin protective alumina film was formed on surface of the alloys.
 - To balance corrosion resistance, age-hardening resistance and ductility, 10 wt.% Cr and 5 wt.% Al containing model is proposed for LFR application [1]
- J.Y. Lim et al. proposed **Fe-Cr-Si system alloy** for high temperature corrosion resistance material. [3]
 - From corrosion test with Fe-Cr-Si system, it verified that Fe alloys with suitable levels of Cr (>12 wt.%) and Si (>2.5 wt.%) will be protected by either a tenacious oxide film or by a low solubility surface region at low oxygen potentials.
 - Experimental result obtained from model alloys after LBE exposure at 600°C demonstrated the film formation process.
 - The hypothesis that Si addition would promote the formation of a diffusion barrier was confirmed by the actual reduction of oxide thickness over time.

Corrosion resistant materials

- Hybrid-layer materials for high temperature LBE application
 - Functionally Graded Composite (FGC)** is devised by MIT which consists of **two layers**, a thin Fe-Cr-Si layer as corrosion-resistance layer, and F91 was chosen as structural layer of the composite for its strength and radiation resistance.
 - By using weld-overlay technique Fe-12Cr-2Si onto F91 billets, co-extruding them and followed by pilgering process, coolant piping and cladding can be produced.

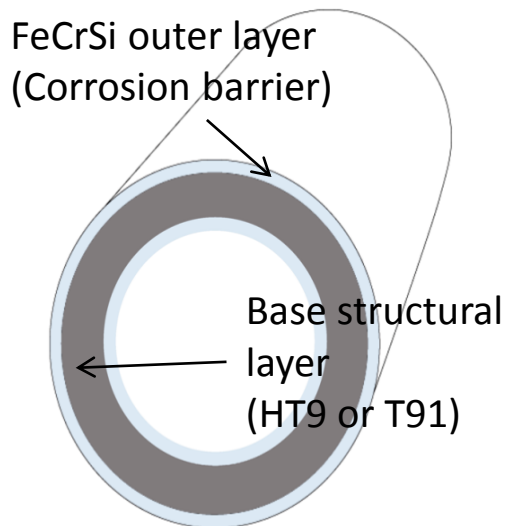


Fig. Schematic diagram of functionally graded composite tube for fuel cladding

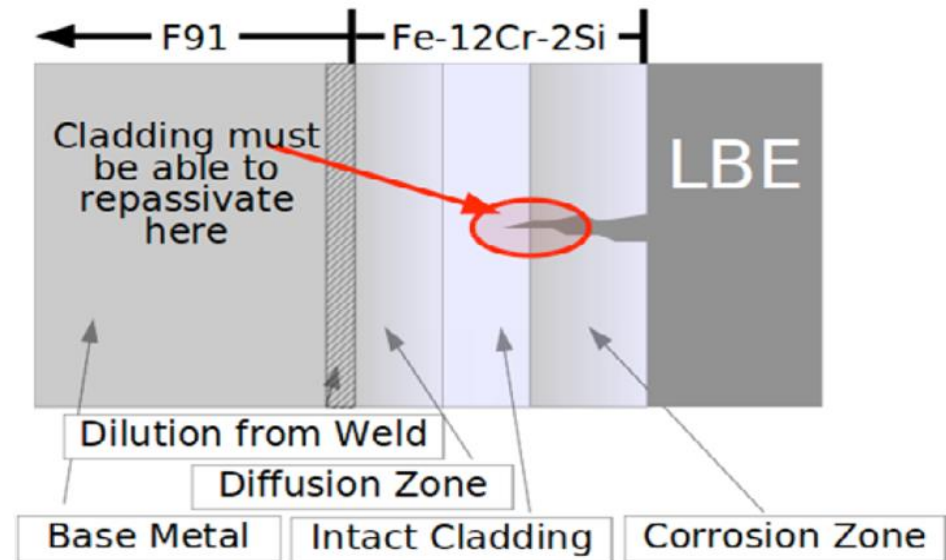


Fig. Diagram showing zones expected to develop during operation of the composite

Objective & Approach

Objective

- The goal of this paper is to further develop the functionally graded metallic composite. This functionally graded metallic composite will ultimately be available to be used as piping and fuel cladding in a lead-bismuth cooled nuclear reactor.
- Optimize the microstructure and mechanical properties of the T91 and Fe12Cr2Si layers in the piping product through heat treatment.

Approach

- Microstructural analysis with
 - ✓ Cross-section analysis with scanning electron microscopy and focused ion beam (SEM & FIB)

Schematic of tube manufacturing process

Procure T91 Billet
10" OD, 2' Long, Wrought A182 Forging Material
T91 (9Cr, 0.1Ni, 1Mo, 0.2V, 0.4Mn, 0.075Nb, 0.4Si, 0.1C, Bal. Fe)

Fuel Cladding
Reduce OD to 9"

Gun Drill 3.25" ID Hole

Weld Overlay 0.5" thick deposit
on OD to make 10" OD.
Material is 12Cr-2Si-Bal. Fe

Reduce OD to 9.940"

Extrusion

Start - 9.940" OD, 3.25" ID, 2'
Finish - 3.75" OD, 3" ID, ~30'

Pipe/Tube Processing

Start - 3.75" OD, 3" ID, 15' x 2 Tubes
Finish - 2" OD, 1.5" ID, 43' x 2 Tubes

Tube (Pilgering)

Start - 2" OD, 1.5" ID, 43' x 2 Tubes
Finish - 0.5" OD, 0.4" ID, 1584'

Finish - 0.5" OD, 50mil Wall, ~5mil Clad

Done

Extruded tube Shipping
MIT → SNU → UNIST

Straightening
(T91, OD clad T91)

Roll deviation: 5mm between roll die
Straightening speed: 15m/min

Extrusion billet
(T91)

OD: 95mm
Thickness: 9mm



Extrusion billet
(OD clad T91)

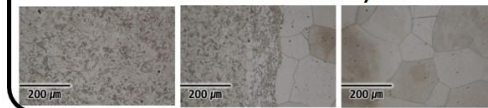
OD: 95mm
Thickness: 9mm



Microstructure analysis



Microstructure analysis



Manual Surface Grinding (Outer surface)
Grinding thickness: < 0.5mm

Pickling

Acid: Sulfuric acid 15% (remove impurities such as oxide)

Cleaning

Water → Acetone → Ethanol

Anticorrosion treatment

Using inhibited oil: P340

1st Pilgering

Thickness: 95mm → 70mm, stroke rate: 13mm/min, feed rate: 6.5mm/min

Condition for Straightening

Ishibashi – 180 Machine

- Number of Roll: 10 (upper roll 5, lower roll 5)
- Roll size: 350mm x 200mm
- Roll spec.: able to 15mm ~ 180mm (OD) able to 1.5mm~ 10mm (thickness)
- Roll deviation: used to 5mm for T91, OD cladding
(generally, copper used 2mm and T91 used 5mm deviation)
- Straightening speed (3m/min)

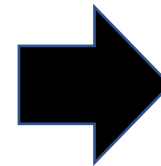


Straightening

- Figures were shown that tube fixed curvature by performing the straightening process.
- The left figure and right figure show the before and after straightening, respectively
- In each figures, left tube is T91, and right tube is OD cladded T91.



Fixed
curvature



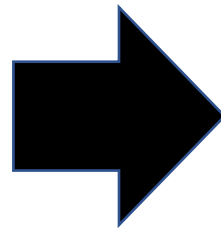
Grinding for T91

- After straightening, the deviations of extruded T91 and OD clad T91 is about 10mm. For the mechanical grinding such as centerless grinding, the deviation of tube have to be under the 2mm. Therefore, extruded T91 have no choice but to manual grinding. (Under the 500 um; as far as possible minimum thickness)

Before Grinding
T91



Fixed surface



After Grinding
T91

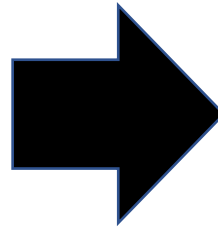


Pickling for T91 & overlay weld OD cladding

- Figures were shown that before and after pickling process. Oxide at surface was removed by pickling at the 15% sulfuric acid.
- For the anticorrosion state, inhibited oil was rubbed on the surface of both tube.

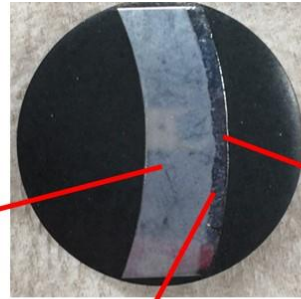


Fixed surface



Cross section of OD clad T91

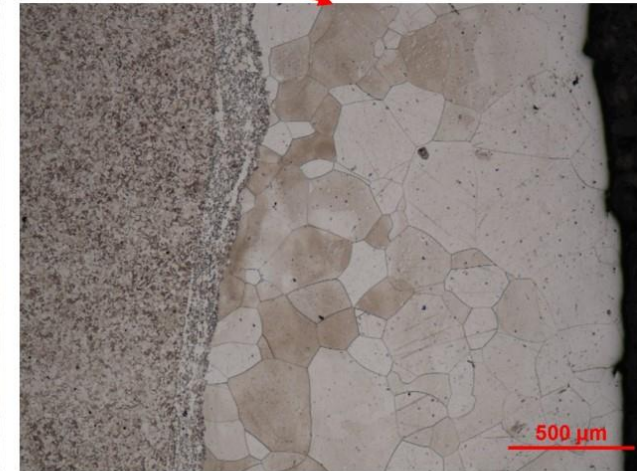
- Figures were shown that microstructure of Fe-12Cr-2Si materials on the OD cladding. The thickness of Fe-Cr-Si layer is 1500 μm (1.5mm).



T91 part



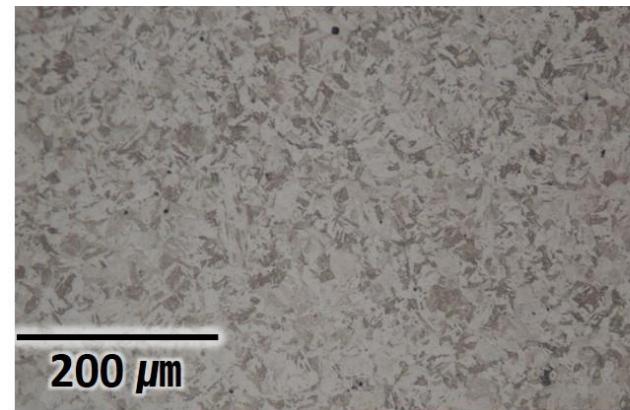
Interaction layer



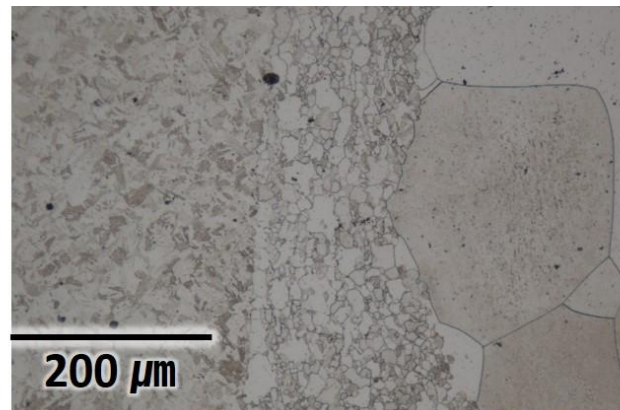
FeCrSi

Cross section of OD clad T91

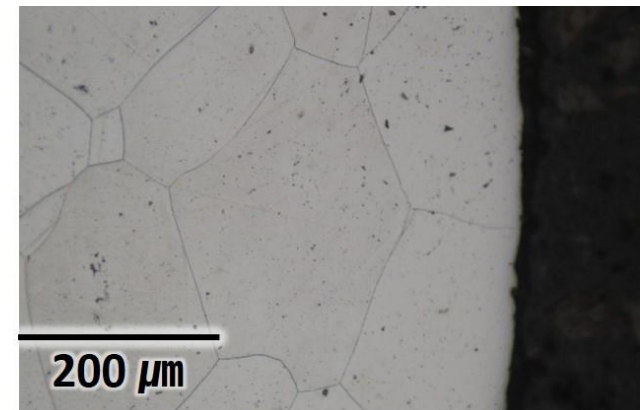
- Figures were shown that microstructure of Fe-12Cr-2Si materials on the OD cladding. In the inner part, it is observed the ferritic/martensitic phase. And, it is observed the prior austenitic grain boundary at FeCrSi.



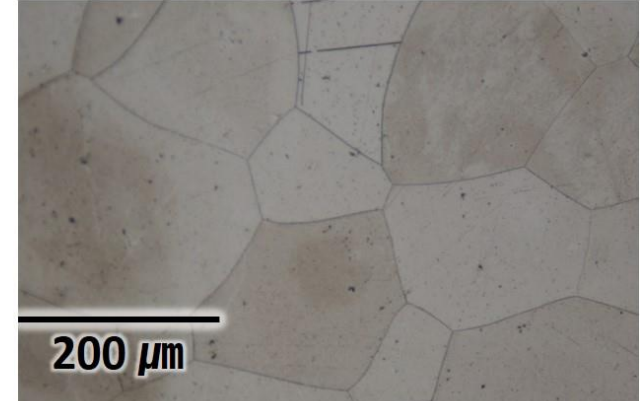
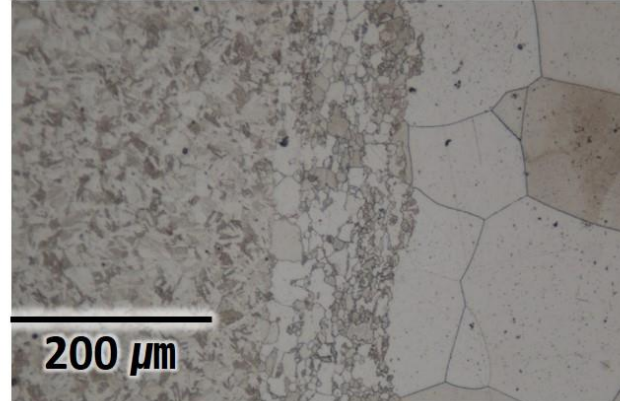
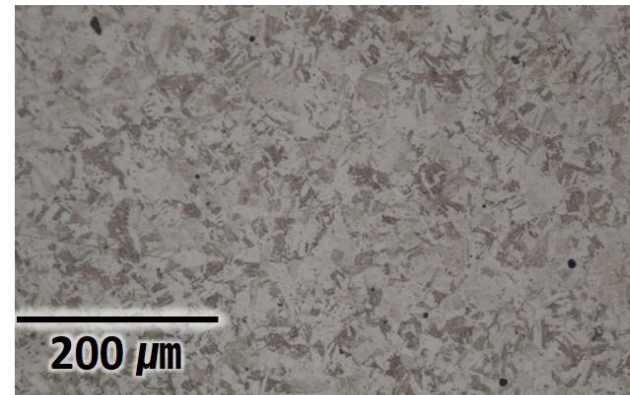
T91 part



Interaction layer

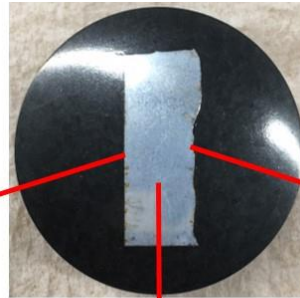


FeCrSi

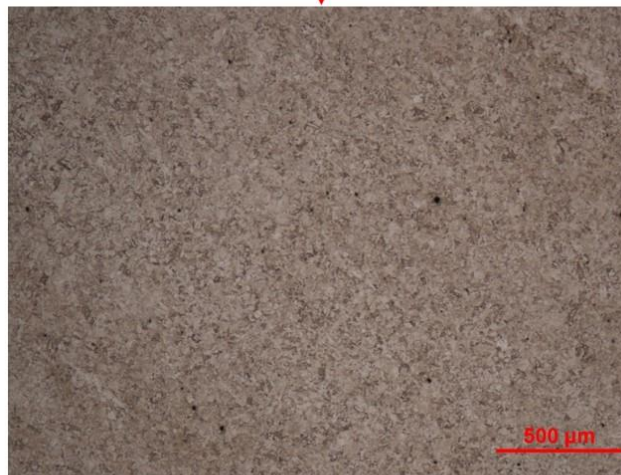


Cross section of T91

- Figures were shown that microstructure of extruded T91 cladding. The thickness of oxide is under the $20\ \mu\text{m}$.



Inner tube layer



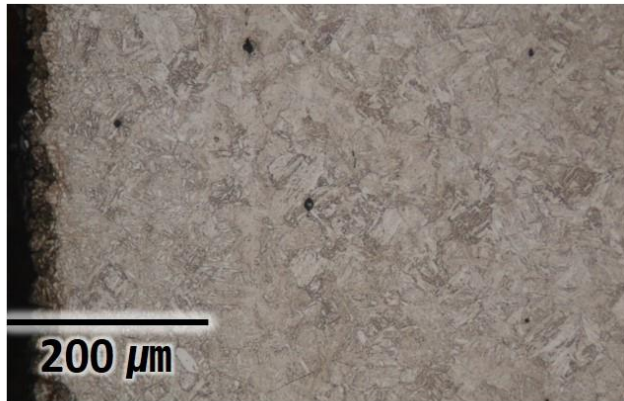
Inside



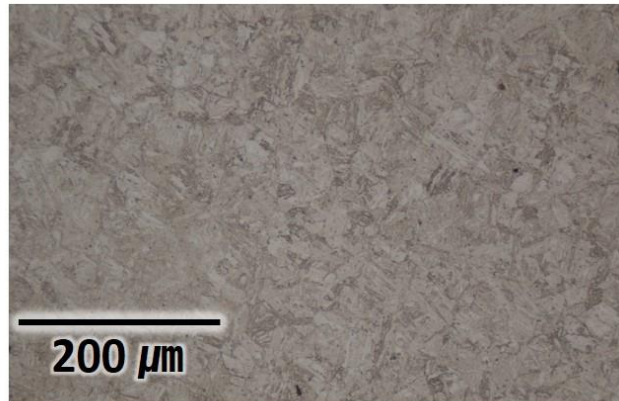
Surface T91

Cross section of T91

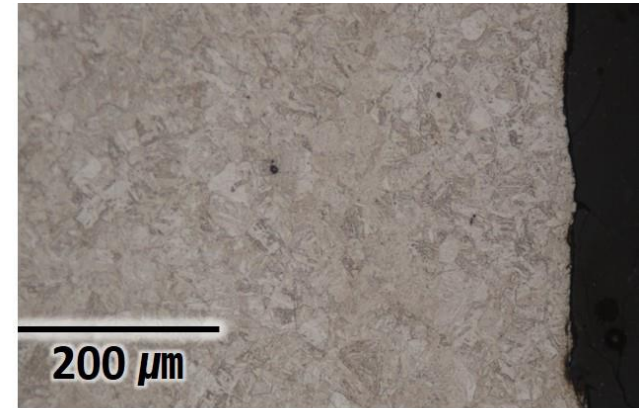
- Figures were shown that microstructure of extruded T91 cladding. The thickness of oxide is under the $20\ \mu\text{m}$. Furthermore, surface of T91 tube has a bad condition.
- The microstructure of T91 are similar with inner part of OD cladded T91.



Inner tube layer



Inside



Surface T91

SEM image

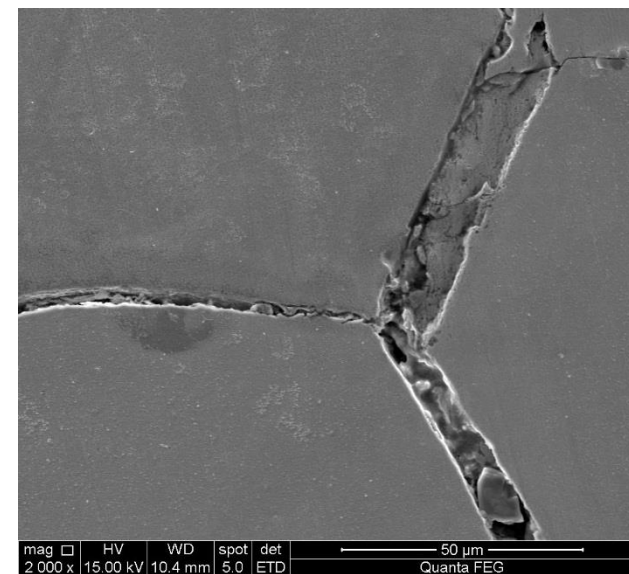
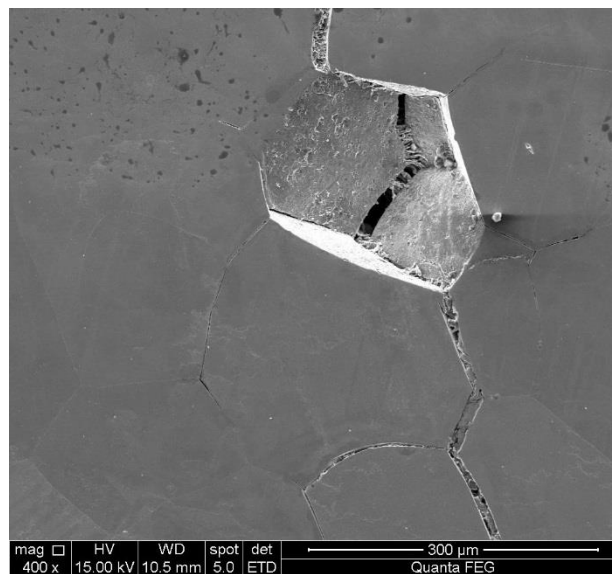
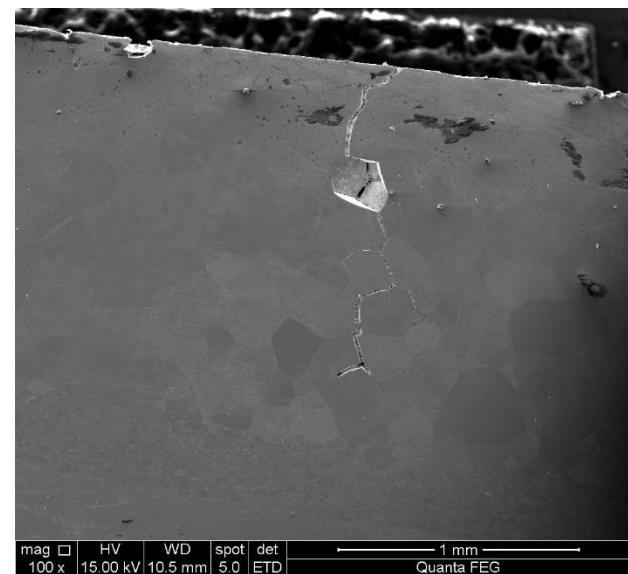
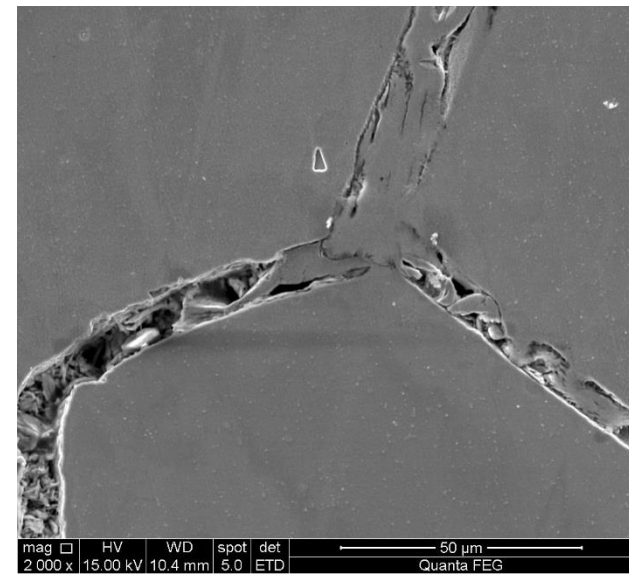
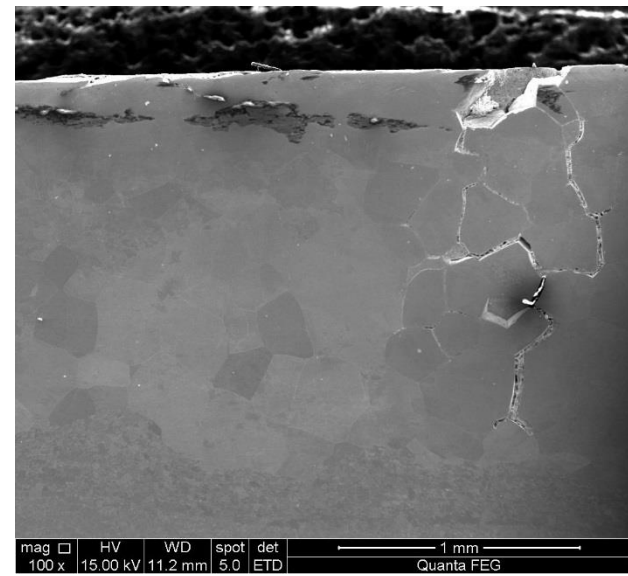


Fig. Crack on OD clad T91 - FeCrSi

EDS mapping (OD cladded T91)

- Figures were shown that EDS mapping of crack of FeCrSi at OD cladded T91.
- There are similar distribution of Fe, Cr, Si in the specimen.
- In those figures, there are some cluster form of silicon. According to literature, Si segregation and silicon rich phase can be formed at high temperature environment.
- There is not observed the significant difference about Mn, S, I, P.
- For the detailed analysis, TEM and dp pattern analysis need to perform.

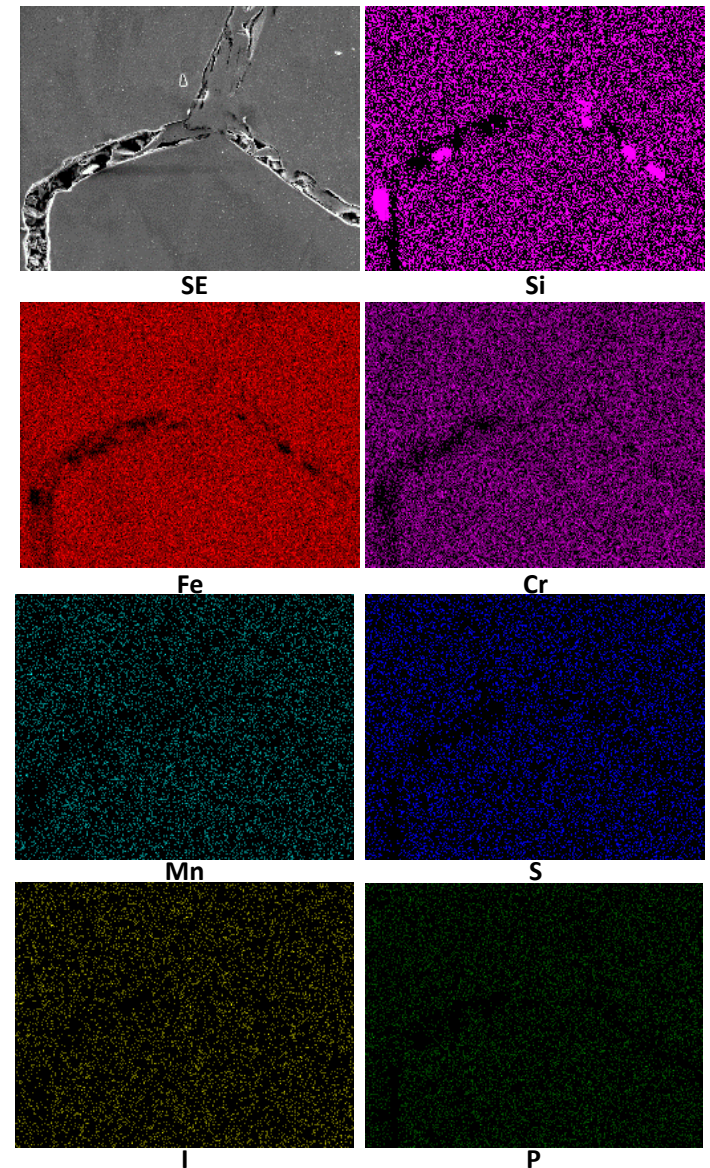
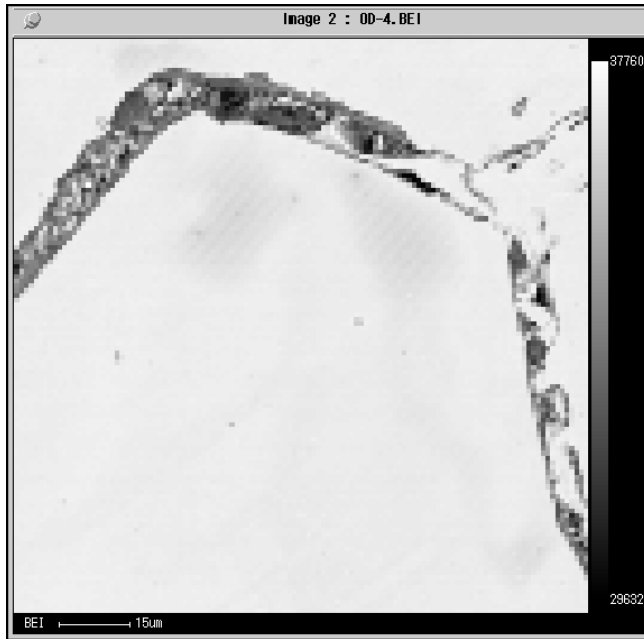
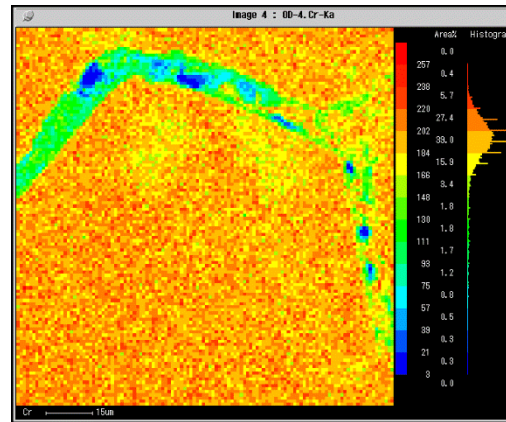


Fig. EDS mapping on Fe-Cr-Si crack

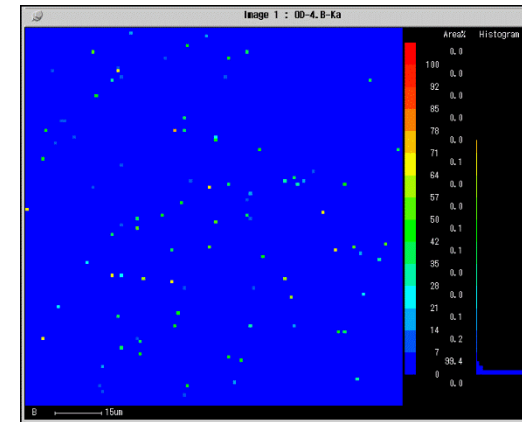
EPMA analysis (OD cladded T91) – additional analysis



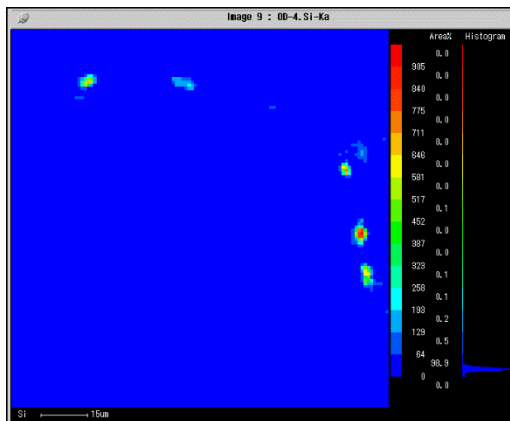
SE



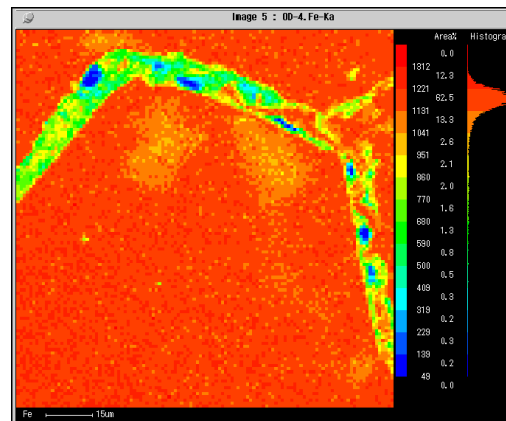
Cr



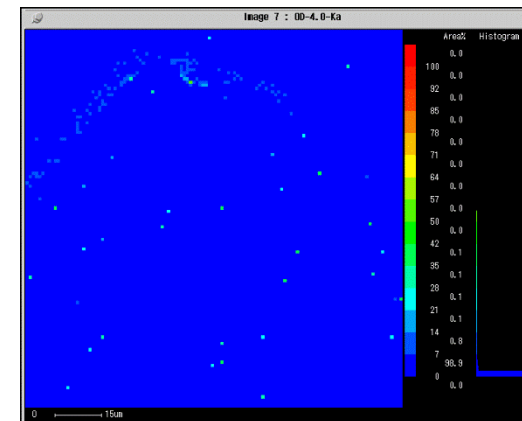
B



Si

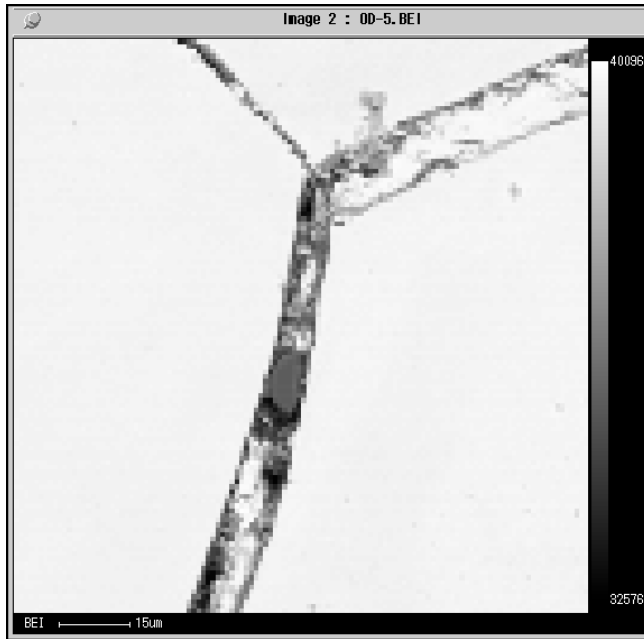


Fe

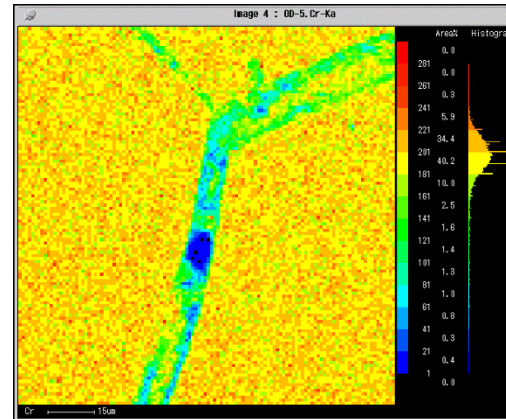


O

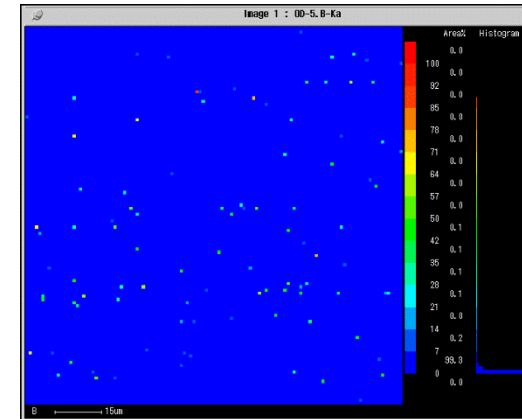
EPMA analysis (OD cladded T91) – additional analysis



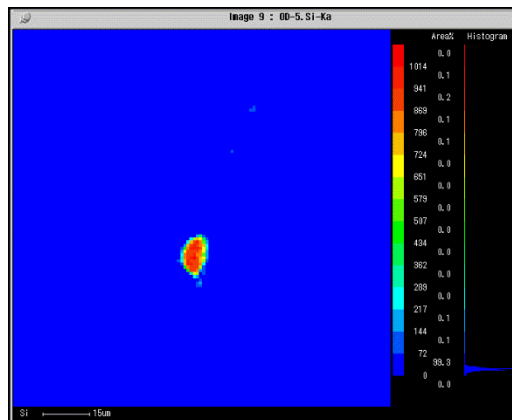
SE



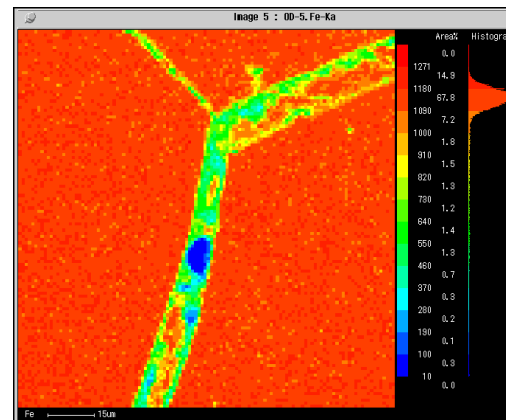
Cr



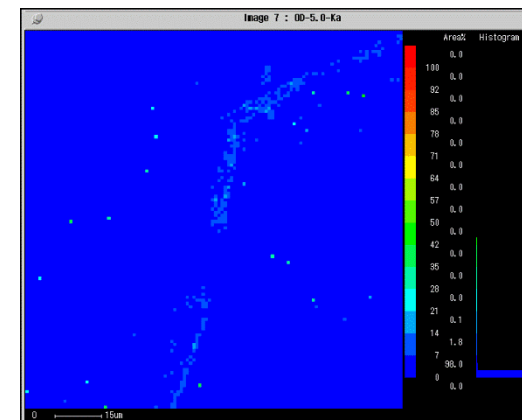
B



Si



Fe



O

Grain boundary segregation

- The temperature dependencies of silicon segregation to both grain boundaries exhibit a maximum near 900 K.
- Both the decrease of silicon segregation at 773 K and a relatively wide in-depth range of the silicon enrichment at all temperatures independent of the values of diffusion length estimates, are found for both grain boundaries.

| Temperature (K) | 1173 | 1073 | 973 | 873 | | 773 | | |
|------------------------------------|------|------|-----|-----|-----|-----|-----|------|
| Time, t (h) | 24 | 24 | 48 | 96 | 120 | 168 | 240 | 1440 |
| $\sqrt{D_{Si}t}$ (μm) | 89 | 34 | 15 | 5 | 6 | 1 | 1.4 | 3.5 |

Fig. Values of silicon diffusivities were calculated from data of Si diffusion.

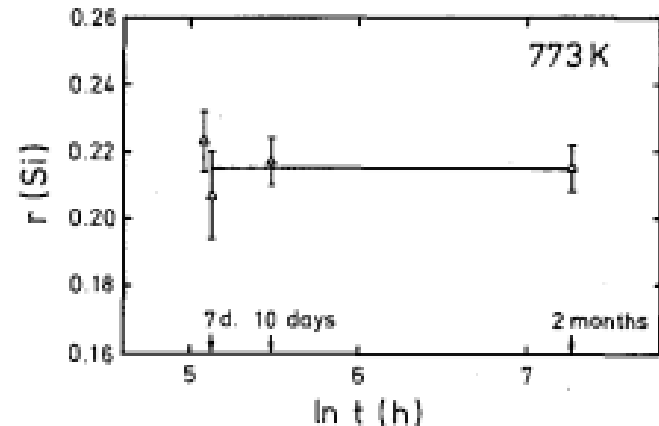
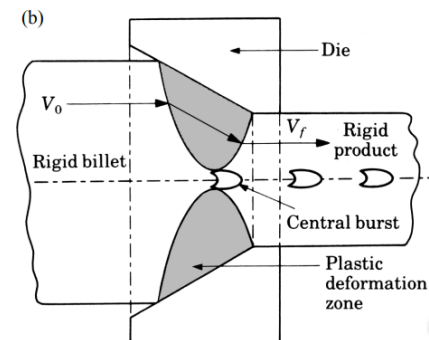
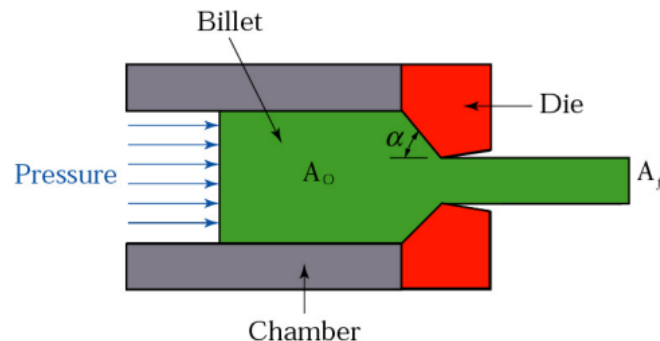


Fig. Dependence of $r(\text{Si})$ on the annealing time at 773K.

Surface cracking by hot extrusion

- Surface cracking by hot extrusion
 - ✓ Longitudinal tensile stresses generated as extrusion passes through the die.
 - ✓ Very high ram speed for the given temperature.
- Internal cracking by hot extrusion
 - ✓ Due to hydrostatic tensile stress at centerline of deformation zone (similar to necking in a tensile test specimen)
 - ✓ Increases with increased die angle, impurities
 - ✓ Decreases with increased extrusion ratio and friction
- If temperature, friction or speed is too high, intergranular cracks occur
- Common in aluminum, magnesium, and zinc alloys
- Bamboo defects are periodic surface cracks that develop due to the extruded product sticking to the die land



Surface cracking by hot extrusion

- Owing to the considerable deformation associated with extrusion operations, a number of defects can occur in extruded products.
- Centerburst is an internal crack that develops as a result of tensile stresses along the centerline of the work part during extrusion. Piping is a defect associated with direct extrusion. It is the formation of a sink hole in the end of the billet. **Surface cracking from high workpart temperatures that cause cracks to develop at the surface. They often occur when extrusion speed is too high, leading to high strain rates and associated heat generation.**

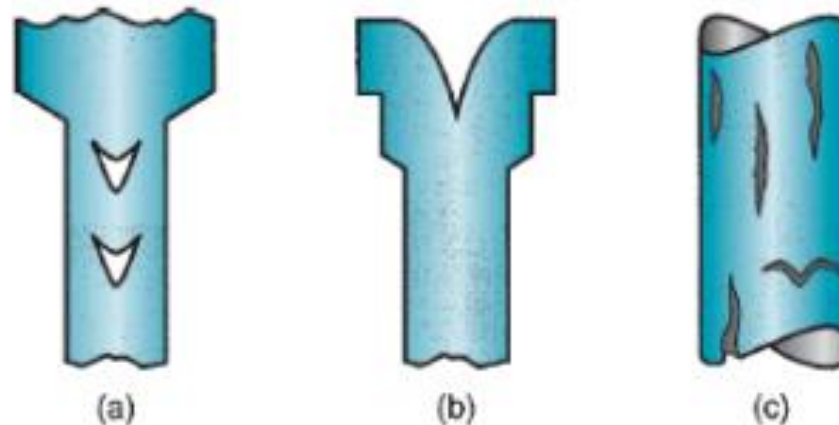


Fig. Common defects in extrusion (a) centerburst, (b) piping, (c) surface cracking

Heat treatment for FGC

- The heat treatment affects the carbide/precipitation phases and microstructures such as type, size, and volume of defects. It plays a decisive role in changing the mechanical properties such as hardness, creep property, and strength.
- According to literature, the austenite grain and ferrite grain might change at temperature higher than 1150 °C because of the dissolution of carbide and precipitation in alloy steel.
- Heat treatment can be improved by removing of carbide/precipitation. Precipitation removes these materials from solid solution, which are thus no longer available for interaction cracking and solid solution hardening. The heat treated specimen will be analyzed.
- Precipitation removes these species from solid solution, and thus they are no longer available for interaction and solid-solution hardening.

Summary

- In this study, microstructure analysis were conducted for investigating the Functionally Graded Composite tube. From this study, the following conclusions are drawn:
 1. Thickness of FeCrSi layer on OD cladding is about 1500 um after hot extrusion.
 2. The microstructure of Fe-12Cr-2Si materials on the OD clad T91 with a small amount of intergranular pores tend to be more prone to grain boundary cracking after hot extrusion processing.
 3. There are key factors for cracking at overlay weld materials. i) Grain boundary segregation ii) Surface cracking by hot extrusion iii) Hot cracking iv) reheat cracking v) crack of overlay weld metal (residual stress)

Thank you for your attention!



UNIST

Study on Q-value about Pilgering Process of Functionally Graded Composite Cladding for Liquid Metal Fast Cooled Reactor Application

Taeyong Kim, Jeonghyeon Lee, Il Soon Hwang, Ji Hyun Kim*

Department of Nuclear Science Engineering
School of Mechanical, Aerospace and Nuclear Engineering
Ulsan National Institute of Science and Technology (UNIST), Ulsan, Republic of Korea
*kimjh@unist.ac.kr

**2018 Heavy Liquid Metal Coolants in Nuclear Technologies (HLMC)
Obninsk, Russia Federation
2018.10.8-10**



Contents

1 Introduction

2 Literature study

3 Model design

4 Conduct analysis & Discussion

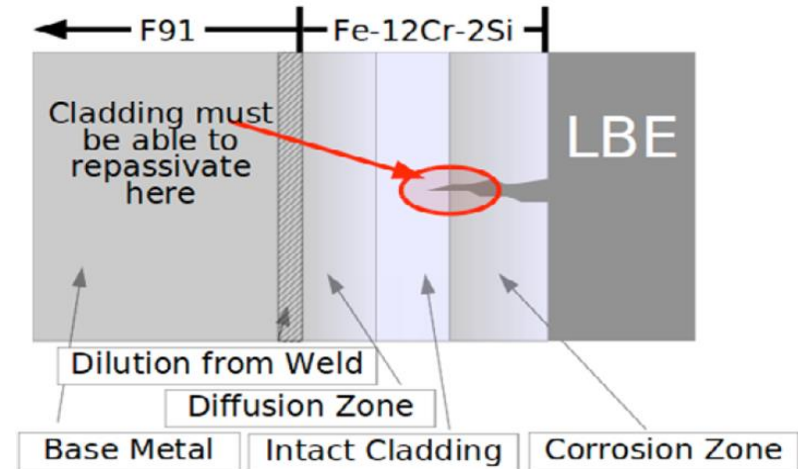
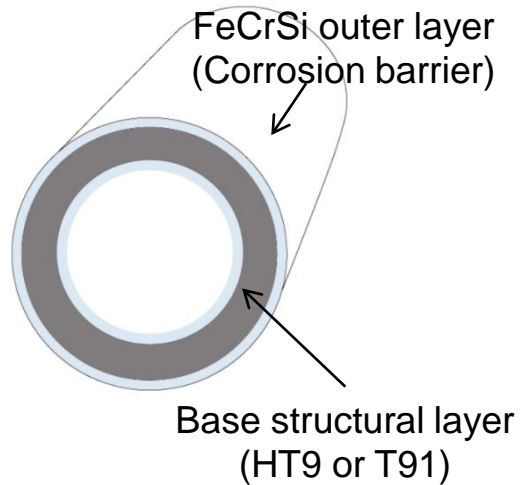
5 Conclusion

1. This work was financially supported by the International Collaborative Energy Technology R&D Program (No. 20168540000030) of the Korea Institute of Energy Technology Evaluation and Planning (KETEP) which is funded by the Ministry of Trade Industry and Energy.

2. This work was supported by the National Nuclear R&D program funded by Ministry of Science, ICT and Future Planning, and by the National Nuclear R&D program (NRF-2017M2A8A1092492) organized by the National Research Foundation (NRF) of South Korea in support of the Ministry of Science, ICT and Future Planning.

Functionally Graded Composite(FGC) Cladding

- Introduction to FGC cladding



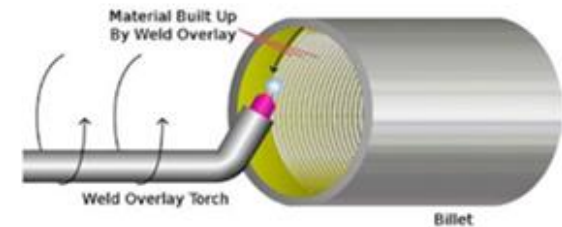
- Manufacturing process of FGC tube

1. T91 TRES billet

4. Co-extrusion

Finish – 95 mm OD, 9.5t

2. Gun drill center hole



3. Fe-12Cr-2Si weld overlay deposit on T91 TRES

5. Pilgering

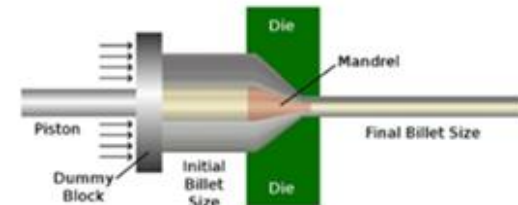




Fig. Pilger machine

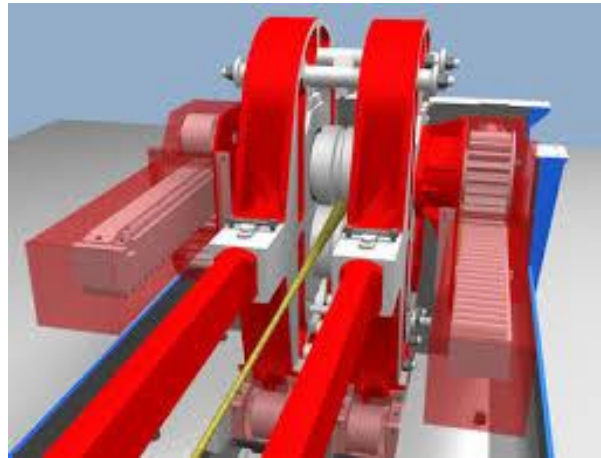


Fig. Schematic of pilger machine

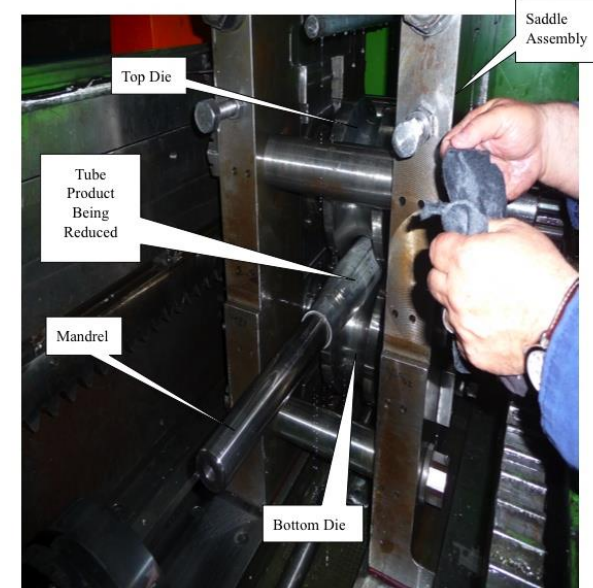
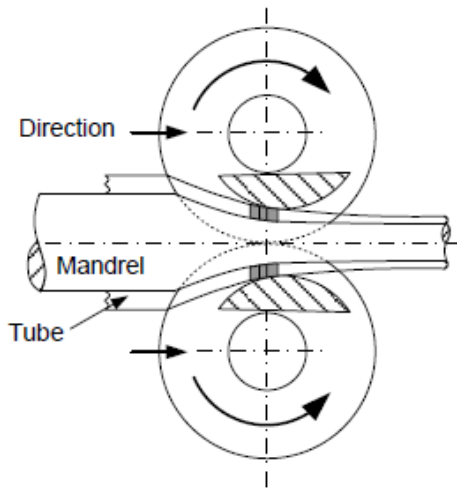


Fig. Schematic for pilgering process

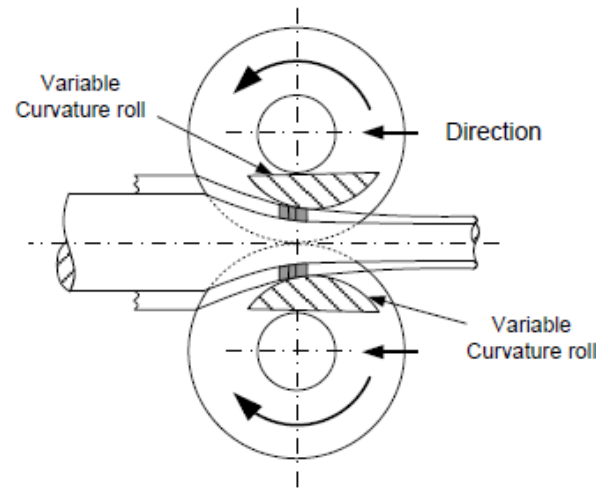
- Cold pilger mill
 - For production of a significant amount of cold rolled tubes, especially **thin-walled**, of **small diameter** from heat resisting, stainless grades as well as alloys on the basis of zirconium, titanium and nickel with increased requirements to **accuracy, quality of finished surface** and **metal structure**
- Vertical Mass Ring Die type mill
 - Varying cross section grooved dies

Outline for Pilger machine tool

- Rolls are attached to the moving rolling stand and they rotate in opposite directions as seen in figure
- The dies groove at the entrance plane is bigger than the diameter of the initial tube while the die groove at the exit is equal to the diameter of the final tube



(a) Forward rolling



(b) Backward rolling

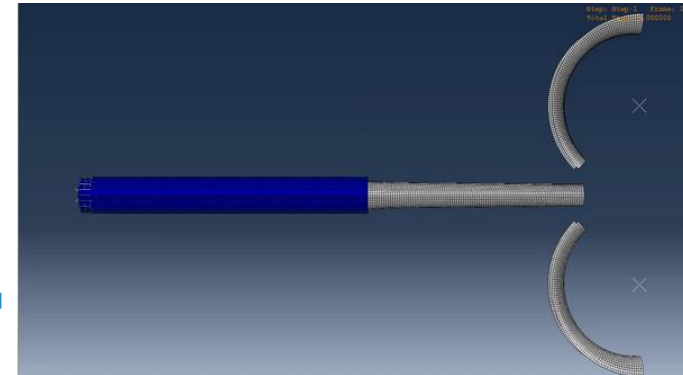
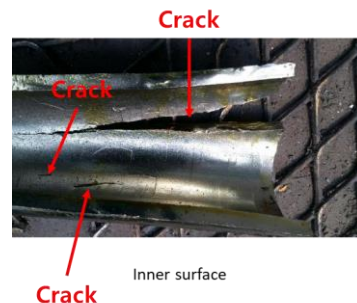
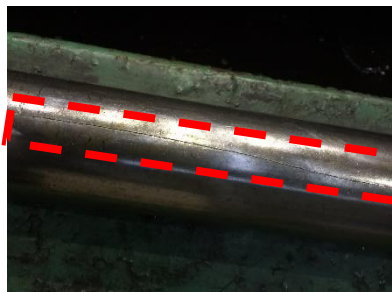


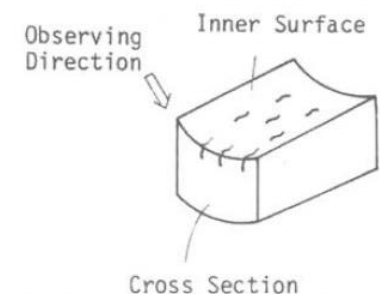
Fig. Side view of the pilger rolling process. Dies rolling without sliding along the mandrel/tube system

Failure of Pilgering Process

| Symptoms | Causes | Suggested Action |
|--------------------------|----------------------------|---|
| Outside diameter defects | CSA reduction to intense | Change tool design so there is a tapering off of strain intensity near the output end |
| | OD reduction too intense | Change tool design |
| | Q factor too high | Change tool design, need smaller relief |
| | Wall reduction too intense | Change tool design |
| Micro cracks on I.D. | Feed rates too high | Change tool design or slow down feed rate |
| | Q << 1 | Change tooling or process |
| | Pickup material on mandrel | Polish mandrel, increase lube |
| | Mandrel too hot | Poor lube filter or lube |



0.12mm



Pilgering process of FGC cladding

- Need
 - Mass production of coated tube

- Limitation
 - Separation between each metallic layer due to overlay-welding process

- Approach
 - Analysis processing factor to manufacture FGC cladding by FEM simulation
 - Stroke/feed rate, reduction rate, **Q-factor**

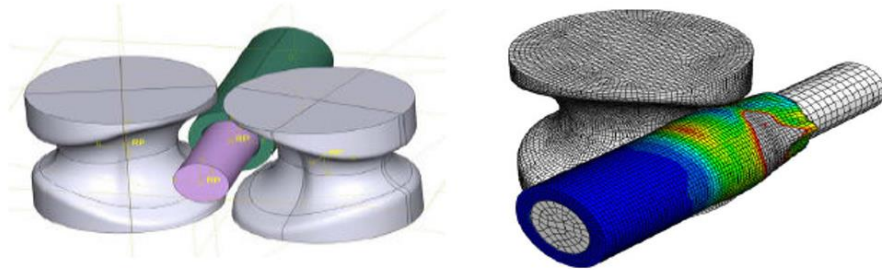


Fig. simulation of pilger process by FEM



Fig. pilger machine(VMR)

Flow chart of steps in framework

1. Identify and define purpose
: variables optimization of FGC pilgering process

2. Search literature and survey experts
: pilgering process, FGC overlay welding, FEM etc...

3. Choose parameters and response
: Q factor, reduction rate etc...

4. Design analysis
: ABAQUS modeling

5. Conduct analysis

6. Integrate data from various source

7. Iterate through steps to continuously improve

8. Apply optimized parameter at actual process

Pilger processing-factors

- Pilger influencing factors
 - Pass schedule
 - Q factor
 - Area reduction rate(=Elongation)
 - Rate parameters
 - Feed rate
 - Stroke rate
 - Heat treatments
 - β -quenching
 - Extrusion preheating
 - Annealing between pilger steps
 - Material
 - Mechanical properties
 - Metallurgical properties

Pilger processing-factors

- Pass schedule

- Q factors

$$Q \text{ factor} = \frac{\ln\left(\frac{OD_{final}}{OD_{initial}}\right)}{\ln\left(\frac{t_{final}}{t_{initial}}\right)}$$

t, T = thickness of tube after, before pilgering

d, D = outer diameter of tube after, before pilgering

- Experiment value
- Ratio of the percentage change in **diameter** to the percentage change in **wall thickness**
- **Q factor greater than one** implies a **small wall reduction** relative to diameter
- Presence of micro cracks on inside diameter of the tube is one of the symptoms of $Q \ll 1$
- This is related with stress flow

- Reduction rate

- is the ratio of the starting tube cross-sectional area to the final tube cross-sectional area
- Although high reduction rate requires few pilgering stage, advantage of that are **superior quality (more uniform, superior microstructure and texture, improved mechanical properties, better surface finish)**, reduction in cycle time as well as manufacturing cost

Technical process

- Rate parameters
 - Feed rate
 - Working distance of tube per stroke by dual track drive when pilger tooling is free of the incoming tube product(cm/#)

 - Stroke rate
 - The cycle number per time(#/min)

 - Productivity takes into account the amount of good product produced
 - Despite of very high rates of production, productivity is very low if the output quality is sub-standard

$$Productivity = (stroke\ rate) \times (feed\ rate) \times (utilization) \times (elongation)$$

- If the process runs at **too high of a feed rate or stroke rate**, the problems such a self feeding, mandrel failure, lube breakdown, marred tools, loss of dimension, bowing, twist can occur

Evaluation of Q factor

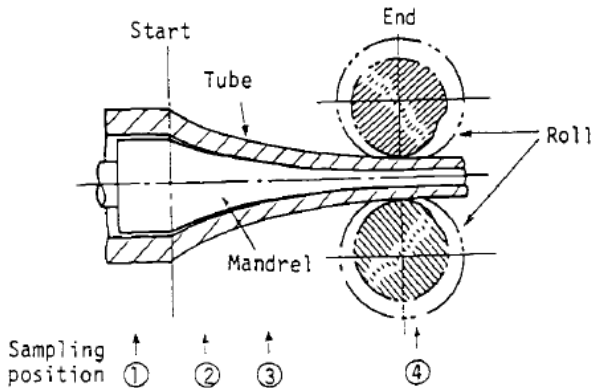
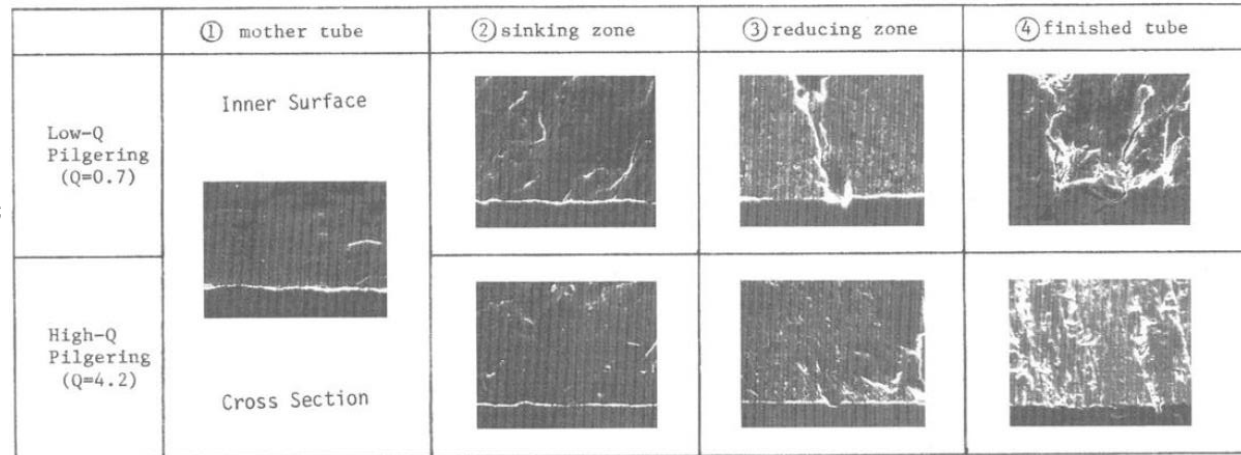


FIG. 7—Tube after intermediate rolling.



10 μm

FIG. 8—Propagation of inner fissures during pilgering.

Micro-wrinkle & Crack propagation

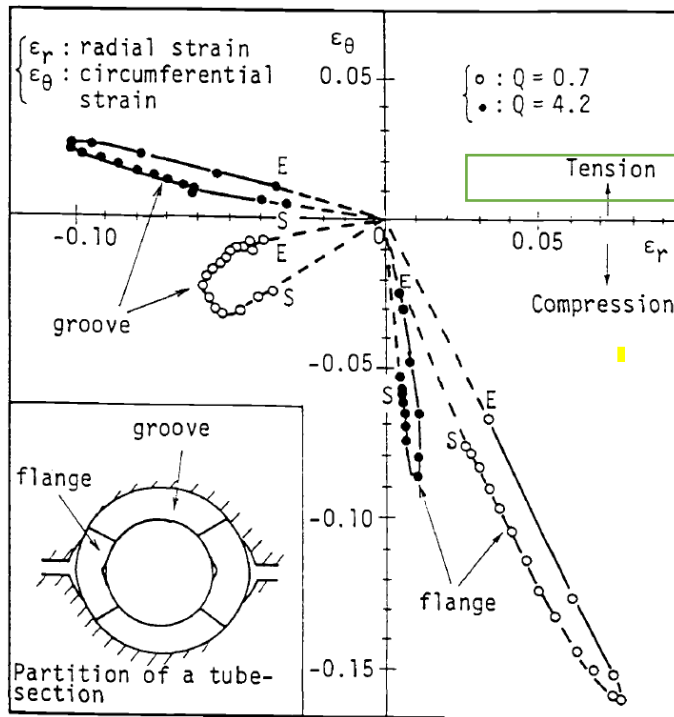
• In the case of low Q values

- ✓ Micro-wrinkles, which form at the sinking deformation zone, are propagated during pilgering. The resulting fissures become deep cracks

• For high-Q values

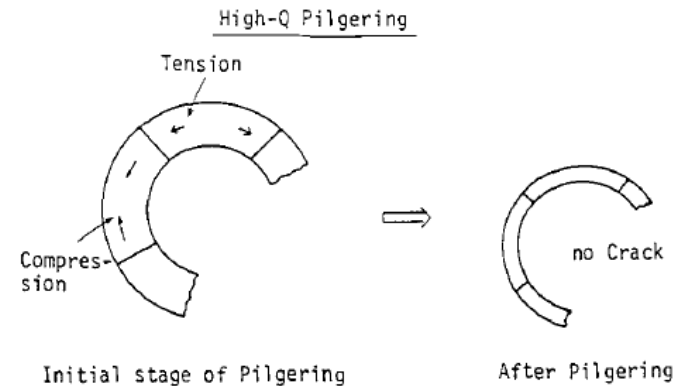
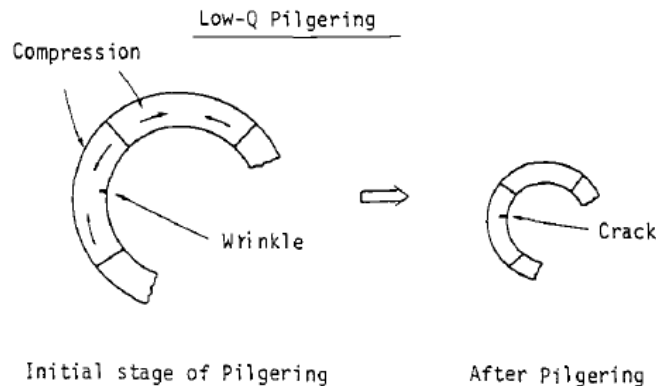
- ✓ Micro-wrinkles at the sinking zone propagate less during pilgering process

Evaluation of Q factor



Method of the plastic deformation model developed by Furugen

- During pilgering process, the tube is rotated to maintain circle shape
- Groove parts are a region directly contacted with dies
- Flange parts partially contact with dies due to side relief
- At low Q-value(0.7),
 - A continual circumferential compressive strain causes wrinkles → propagate → crack
- At high Q-value(4.2),
 - It refrains from cracking because it is both a compressive and a tensile strain



Mechanical properties

- To analyze pilger process, the mechanical properties of materials **are required**

| Property | Density (g/cm ³) | Young's modulus (GPa) | Poisson's ratio | Yield strength (MPa) | Tensile strength (MPa) |
|----------|---------------------------------|--------------------------|-----------------|-------------------------|---------------------------|
| FeCrSi | 7.76 | 180.1 | 0.31 | 253.8 | 386.5 |
| T91 | 7.75 | 214.5 | 0.33 | 195.9 | 312 |

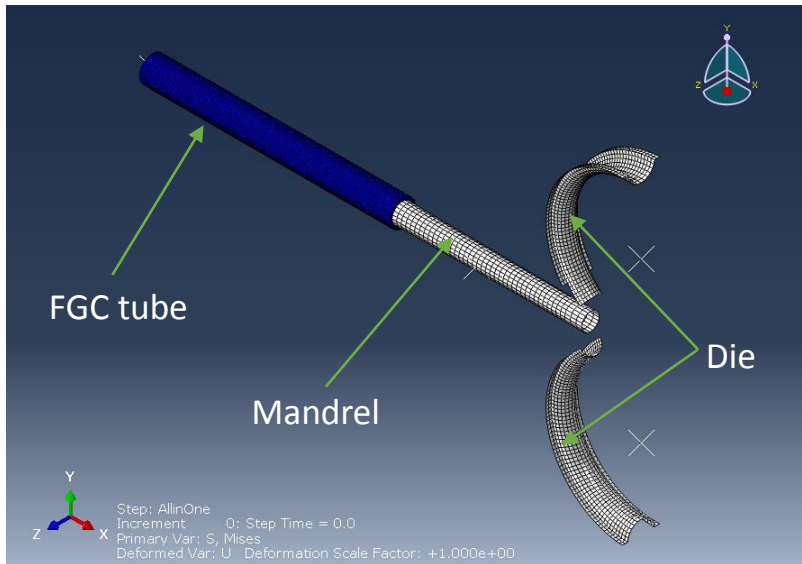


Fig. Geometry Model for pilgering process simulation with VMR50

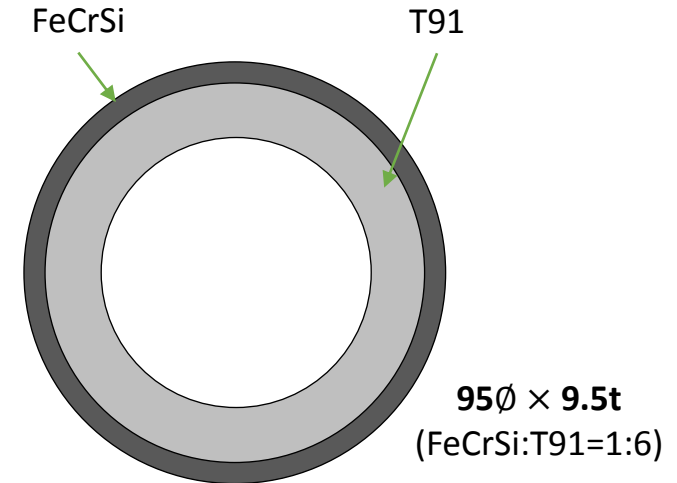
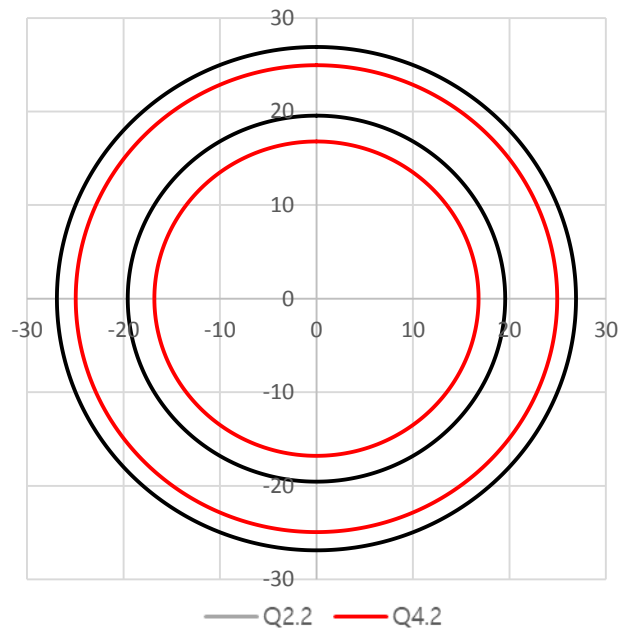


Fig. Cross section of FGC tube

- The geometry model for pilgering process simulation is composed of FGC tube and VMR tool(mandrel and two dies)
- The ratio of FeCrSi thickness to T91 thickness is 1/6
 - It comes from final ratio of FeCrSi/Cr thickness

- Q-factor control

| | Step 1 | Step 2 | Reduction rate | Q value |
|--------|------------------------------|---------------------------------|----------------|---------|
| Case 1 | 95 \emptyset \times 9.5t | 53.8 \emptyset \times 7.34t | 58 % | 2.2 |
| Case 2 | (FeCrSi:T91=1:6) | 49.9 \emptyset \times 8.15t | 58 % | 4.2 |

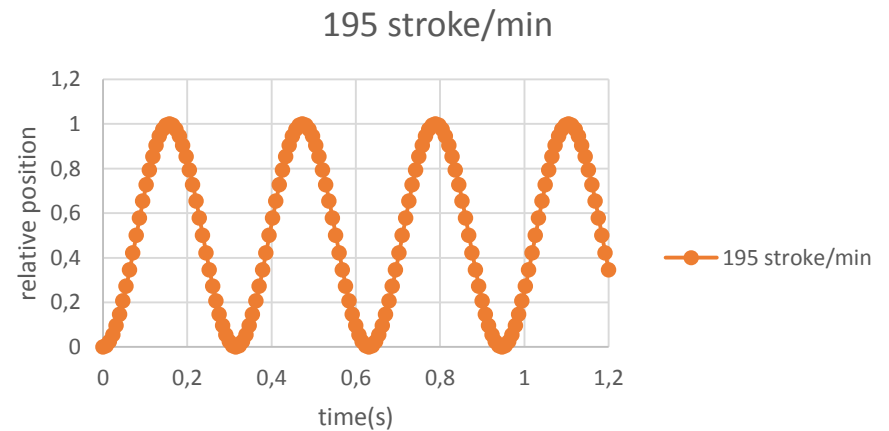
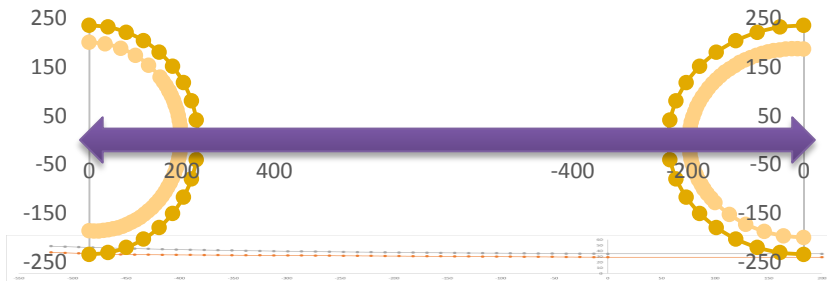


Pilgering Plan

- Fixed variables
 - Tools (VMR125)
 - Turning angle : $\frac{1}{4}$ rotation

- Control variables
 - Frictional coefficient with stroke rate 195 #/mm and feed rate mm/stroke
 - $\mu=0.1$

 - Rate factors
 - Stroke rate : 195 #/min
 - Feed rate : 9 mm/stroke



Strain Evaluation at Outer Surface

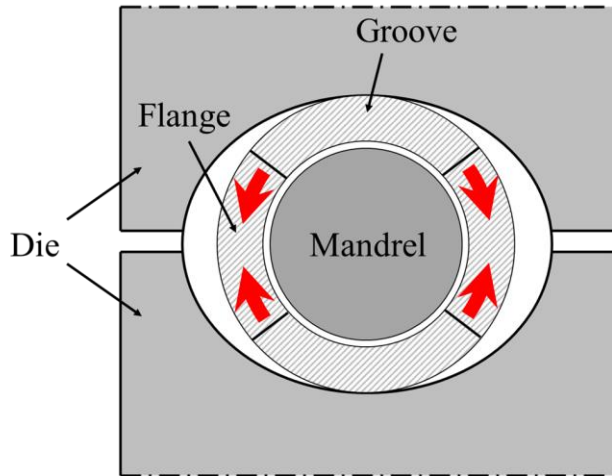


Fig. Cross-section of pilgering tool

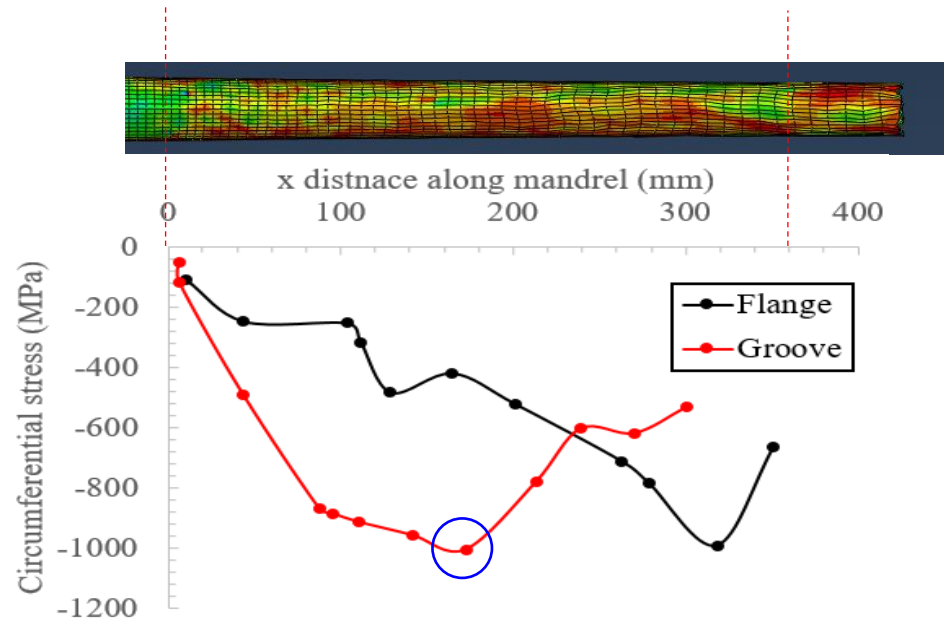


Fig. Distribution of circumferential stress along mandrel(Q=2.2)

- At position on 194 mm of mandrel
 - Die was directly contacted, and a high compressive stress was generated at about 190 mm for the weak groove, so the analysis was carried out at that part

Strain Evaluation at Outer Surface

Table. Case study about Q=2.2 and 4.2

| | Step 1 | Step 2 | Q value |
|--------|------------------------------|---------------------------------|---------|
| Case 1 | 95 \emptyset \times 9.5t | 53.8 \emptyset \times 7.34t | 2.2 |
| Case 2 | (FeCrSi:T91=1:6) | 49.9 \emptyset \times 8.15t | 4.2 |

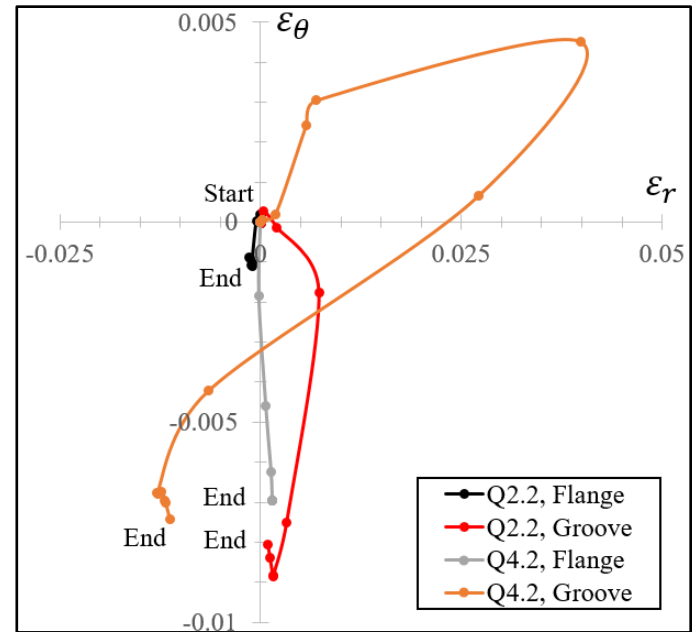


Fig. Distribution of circumferential and radial strain on 194 mm of mandrel at Q=2.2 and 4.2

■ Strain distribution analysis

- Through the results of the strain calculation in the circumferential and radial directions, the flange part shows compressive strain in the circumferential direction. In the grooved section, the circumferential strain in the Q-value of 4.2 was compressive after stretching, whereas in the Q-value of 2.2, there was only compression for the circumferential strain.
- The results show that there is a risk of crack growth if the Q-value is less than 2.2 when sustained pressure is applied.
- However, the Q-value of 4.2 seems to reduce crack growth by repeatedly compressive and tensile strain.
- In addition, the strain in the radial direction increases in the groove, which is reduced because the die increases while pushing the tube and decreases after passing

Conclusion

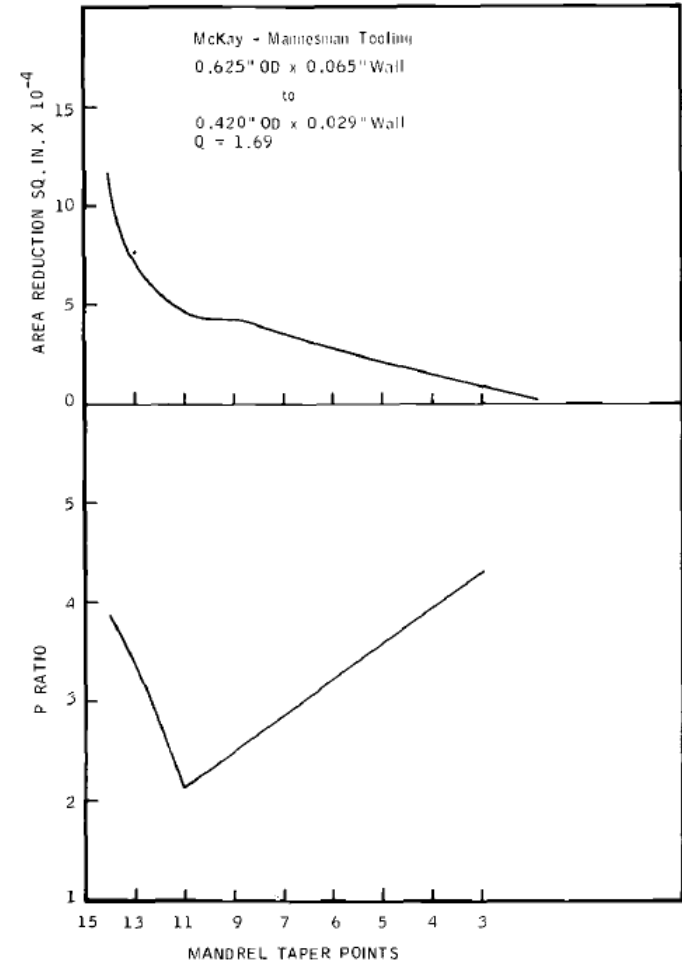
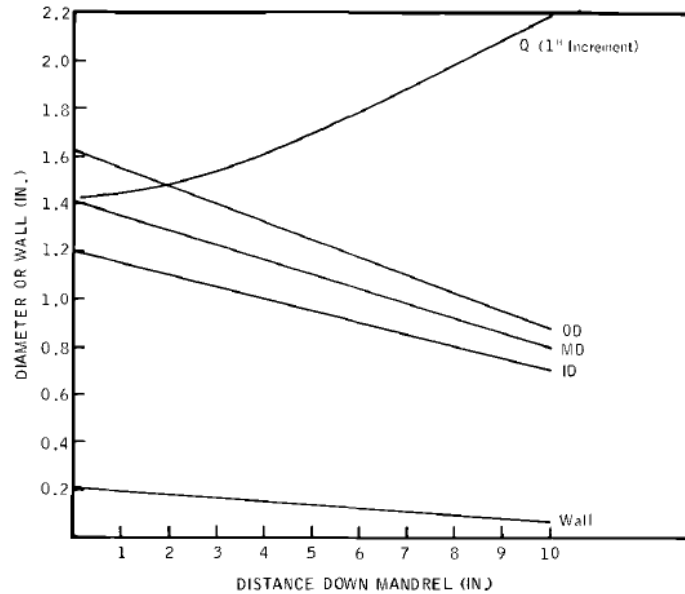
- In this paper, pilgering process simulation of FGC tube is analyzed. The result is the case study by using conventional stroke and feed rate at VMR 125 pilgering machine
- **Evaluation of strain distribution**
 - The strain was calculated in the circumferential and radial directions with different Q-values.
 - In Q-value 2.2, there is a risk of crack growth due to compressive strain in both the flange part and the groove part.
 - On the other hand, in the high Q value of 4.2, tensile is generated in the groove part, it seems to be beneficial to the process.
- **Future work**
 - Until now, Q value was analyzed at outer surface(FeCrSi layer). Strain distribution at inner surface will be also evaluated with various Q value.
 - Moreover, the double layer composite has interface which is vulnerable to difference strain change of each layer.
 - It will be important point to prevent spallation of each layer, considering longitudinal strain.
 - Complex adjustment of Q value will be required.

Thank you for your attention!



UNIST

Updated Q factor; P ratio

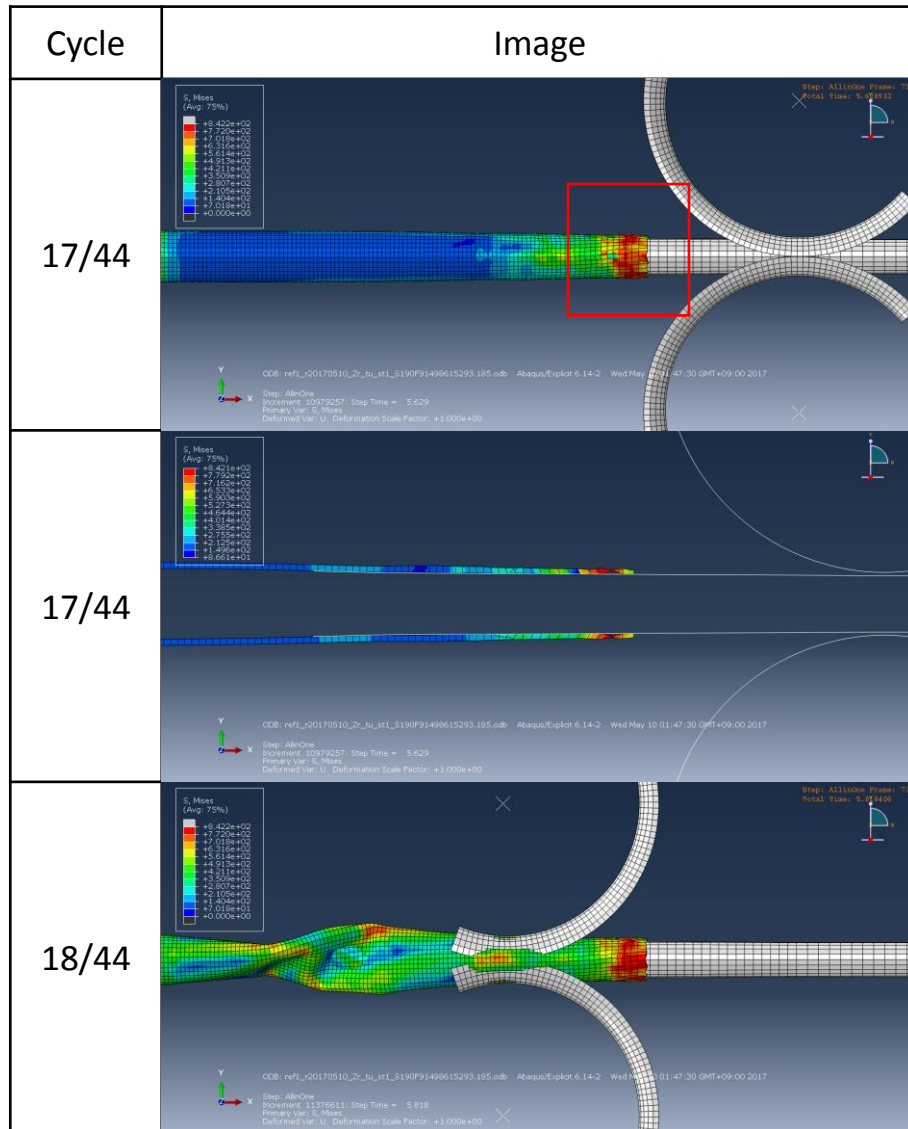


- Q factor only has 4 variables; 2 thickness+2 diameter
- Therefore, instantaneous ratio at a point can't be replaced
- So, there is P parameter by using mean diameter

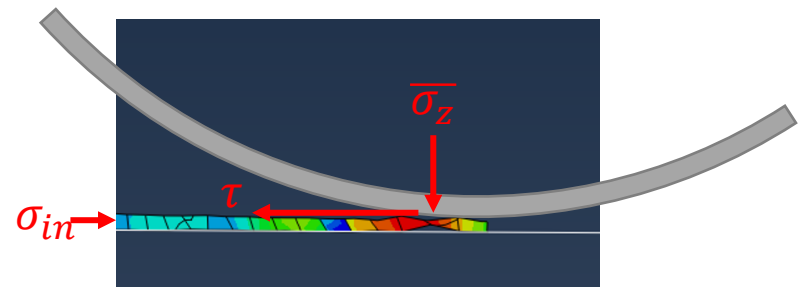
$$P = \frac{\frac{dW}{W}}{\frac{dMD}{MD}} = \text{constant}$$

Case study – Frictional coefficient

- $\mu=0.3$



- There is highly distorted region at head of the tube
- Because the highly slipped region is impacted by high force which is resulted from
 - Frictional coefficient(μ)
 - Reduction rate(r)



Assum that $\sigma_{in} = 0$,

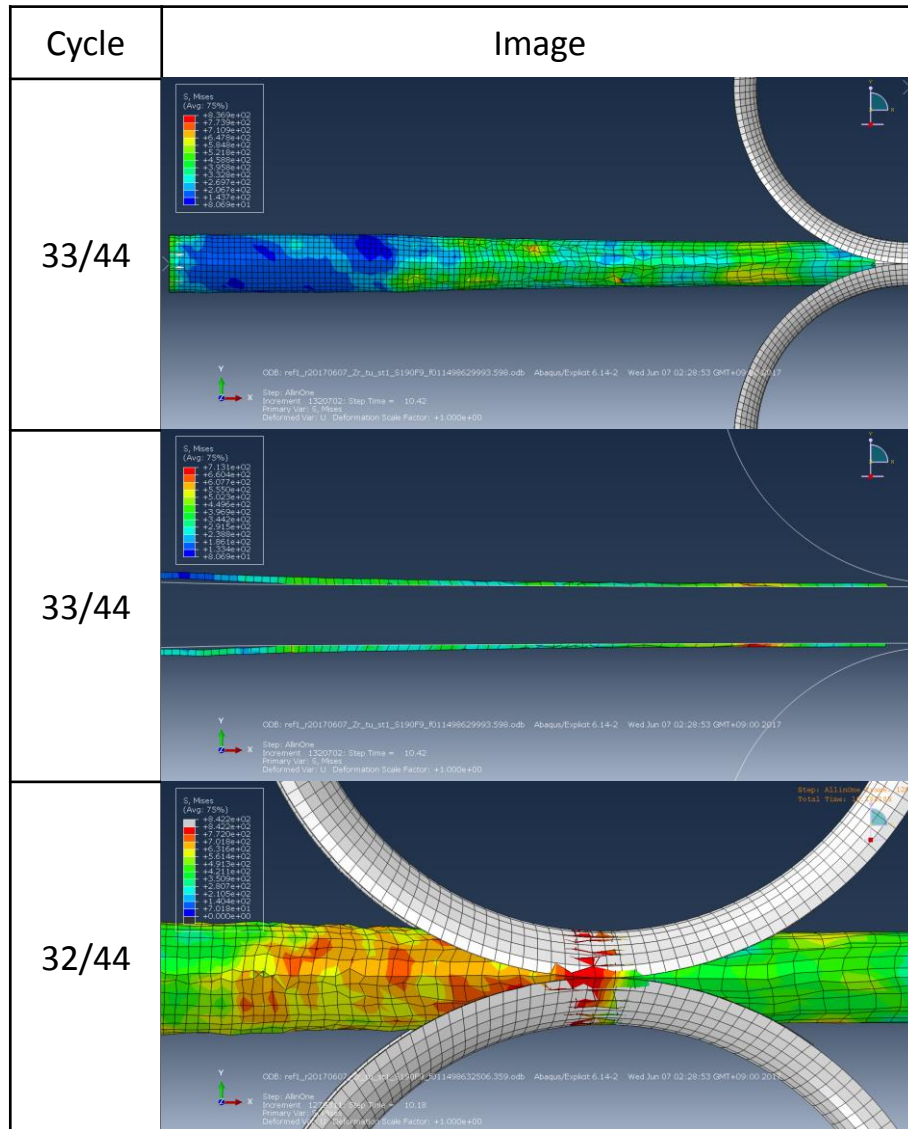
$$\tau_{zx} = \mu \cdot \bar{\sigma}_z = \mu \cdot (k \cdot \bar{\epsilon}^n) = \mu \cdot \left\{ k \cdot \left(\frac{\sum r_i^n}{N} \right) \right\}$$

If $\tau_{zx} > \tau_{critical}$, fail

- Finally, the tube is tightened by high frictional force and the distorted region with mandrel

Case study – Frictional coefficient

- $\mu=0.1$



- Low friction coefficient gives relatively uniform stress/strain distribution
- However, a few discontinuous region appears because of low density of mesh
- Slip of tube is reduced comparing with high frictional force model. Nevertheless, there is a slight slip
- It means that slip of tube is related to not only frictional coefficient but also
 - Reduction rate
 - Slip factor
 - Stroke rate(=stroke speed)
- Also, we can observe that tube is protruded from side edge of die
- Therefore, lower feed rate is useful to perform pilgering process

**RESEARCH OF PIPES FROM STEEL 09MN2SI
TO OBTAIN THE CHARACTERISTICS
NECESSARY TO ASSESS THE STRENGTH,
SAFETY AND LIFETIME OF THE BREST-OD-300
REACTOR UNIT**

JSC RPA «CNIITMASH»
Logashov S.U., Orlov A.S.,
Gavrilov E.V., Khaymin S.V.



Государственный
научный центр РФ
ЦНИИТМАШ



This work was carried out within the framework of the Federal Target Program "Nuclear Energy Technologies of the New Generation for the Period 2010-2015 and for the Future to 2020" for the development and manufacture of the BREST-OD-300 reactor plant.

Seamless hot-formed pipes of 09Mn2Si steel and their welded joints are used for manufacture of the reactor vessel heating system BREST-OD-300.

The aim of this development was to obtain the insufficient data necessary to justify service characteristics used in the evaluation of the strength, safety and lifetime of seamless hot-formed pipes of 09Mn2Si steel and their welded joints intended for the construction of structural elements of the reactor vessel heating system BREST-OD-300.

Within the framework of the development, tests by definition values of creep-rupture strength and ductility for the metal of pipes of 09Mn2Si steel and their welded joints at operating temperatures were done.

The test program "Testing for the justification of the application of pipes of 09Mn2Si steel for elements of reactor vessel heating system BREST" is designed taking into account the requirements of the PNAE G-7 002-86, PNAE G-7 008-89, NP-089-15 [1,2,3] and covers the following types of tests by definition:

- calculated values (average) of physical characteristics: coefficient of linear expansion, coefficient of thermal conductivity, density, specific heat of metal pipes in the operating temperature range and at the temperatures of violation of normal operating conditions and emergency conditions;
- calculated values of mechanical properties (R_m , $R_{p0,2}$, A_5 , Z) for the base metal of pipes and welded joints in the operating temperature range and at the temperatures of violation of normal operating conditions and emergency conditions;
- the influence of thermal aging of the metal of pipes and their welded joints on the calculated values of mechanical characteristics (R_m , $R_{p0,2}$, A_5 , Z) for a resource on the basis of tests of not less than 20 000 h (with the testing of samples after 10 000 and 15 000 h) at operating temperatures;
- calculated values of creep-rupture strength () for the metal of pipes and their welded joints, and ductility (δ), creep-rupture and isochronous creep curves (deformation up to 3%) for the metal tubes based on tests of at least 20,000 h with extrapolation to 260 000 h at operating temperatures.

And tests by definition values of creep-rupture strength and ductility on limited time base were done.

Within the framework of this development, representative lot of seamless hot-formed pipes from 09Mn2Si steel of the same standard sizes, made according to the same normative documents (TU 14-3R-1128-2007) and as pipes intended for the structural elements of the reactor vessel heating system BREST-OD-300, was purchased. These pipes was manufactured by:

- PJSC «Sinara pipe factory»;
- PJSC «Seversk pipe factory».

Certification data of mechanical properties of representative lot of hot-formed pipes at normal temperature

| Yield strength ($R_{p0.2}$), N/mm ² | Ultimate strength (R_m), N/mm ² | Relative extension (A_5),% |
|---|--|-----------------------------------|
| 385-435 | 520-565 | 29-39 |

Welded joints were made by semi-automatic arc welding with copper-plate wire HENDERHCW-50AER70S-6 (Sv-08G2S-O) with a diameter of 0.8 mm in accordance with GOST 2246-70 in protective gas (argon). Welding was carried out in accordance with the instruction № ТКДВ.25291.00033.

Certification data of chemical composition and mechanical properties of welding wire presented in Table 2 and 3.

Certification data of chemical composition of welding wire

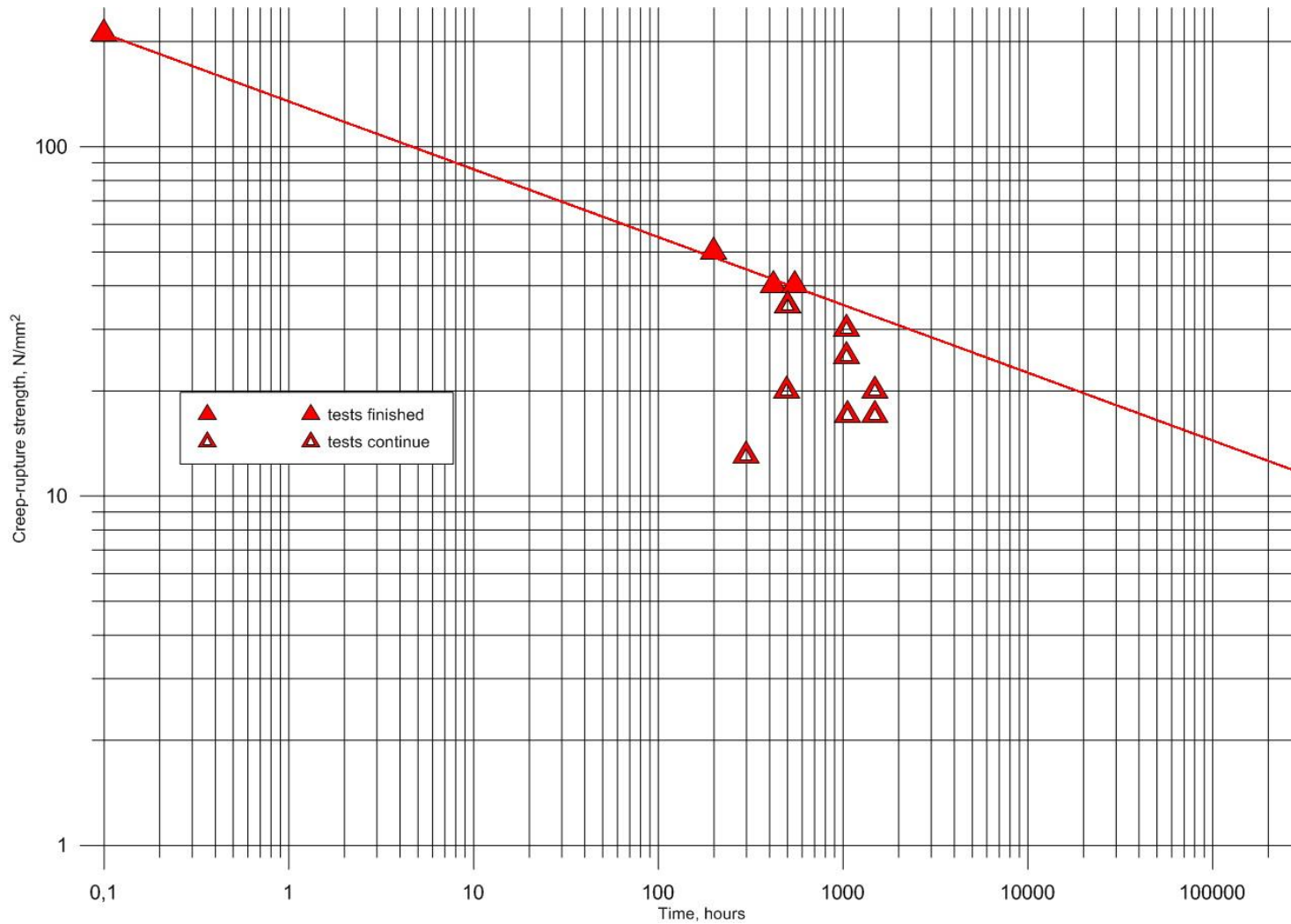
| | C | Si | Mn | Cr | Ni | Cu | S | P |
|--------------|------|------|------|----|----|------|-------|-------|
| SV-08Mn2Si-0 | 0,08 | 0,88 | 1,53 | - | - | 0,21 | 0,011 | 0,011 |

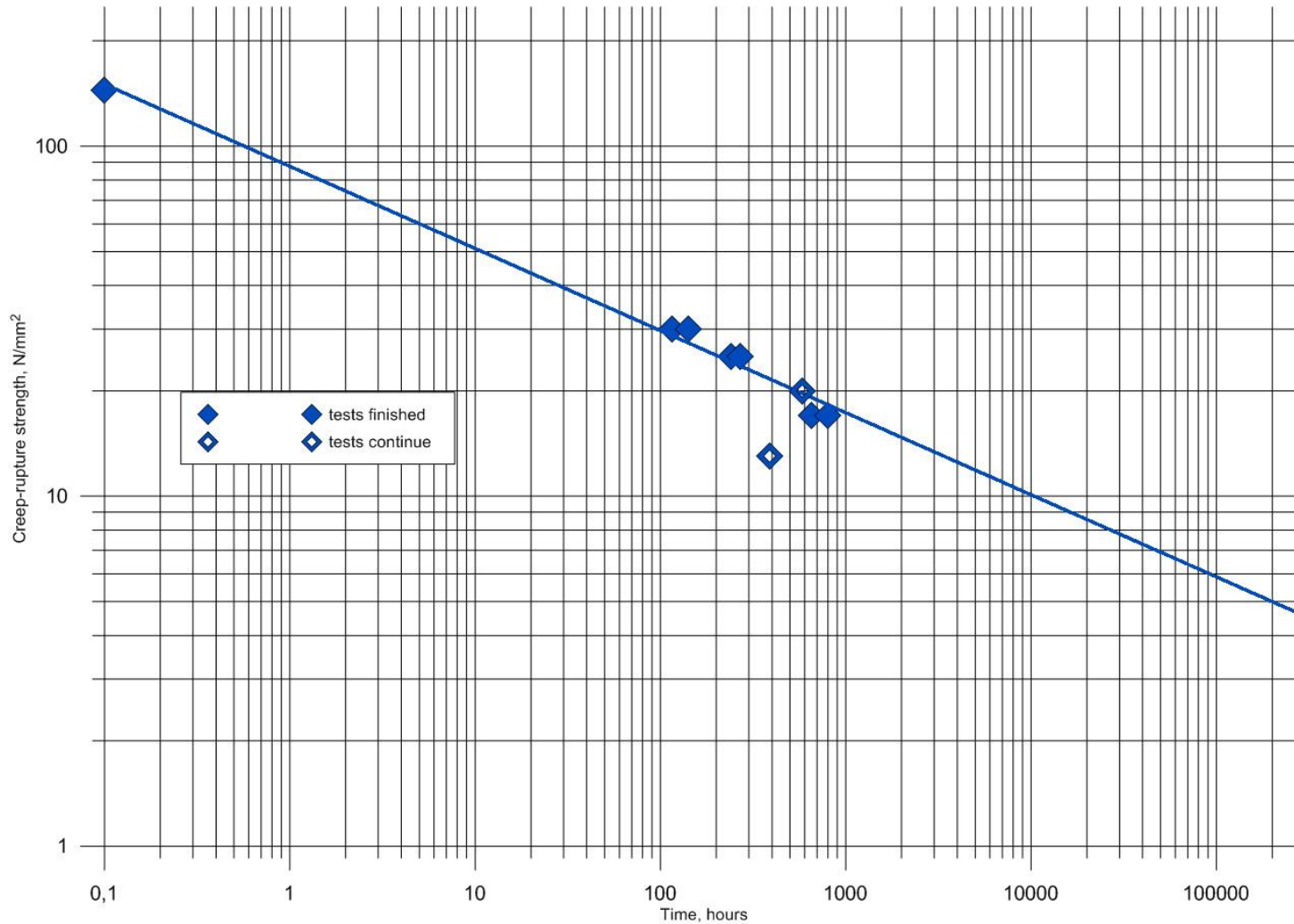
Certification data of mechanical properties of welding wire at normal temperature

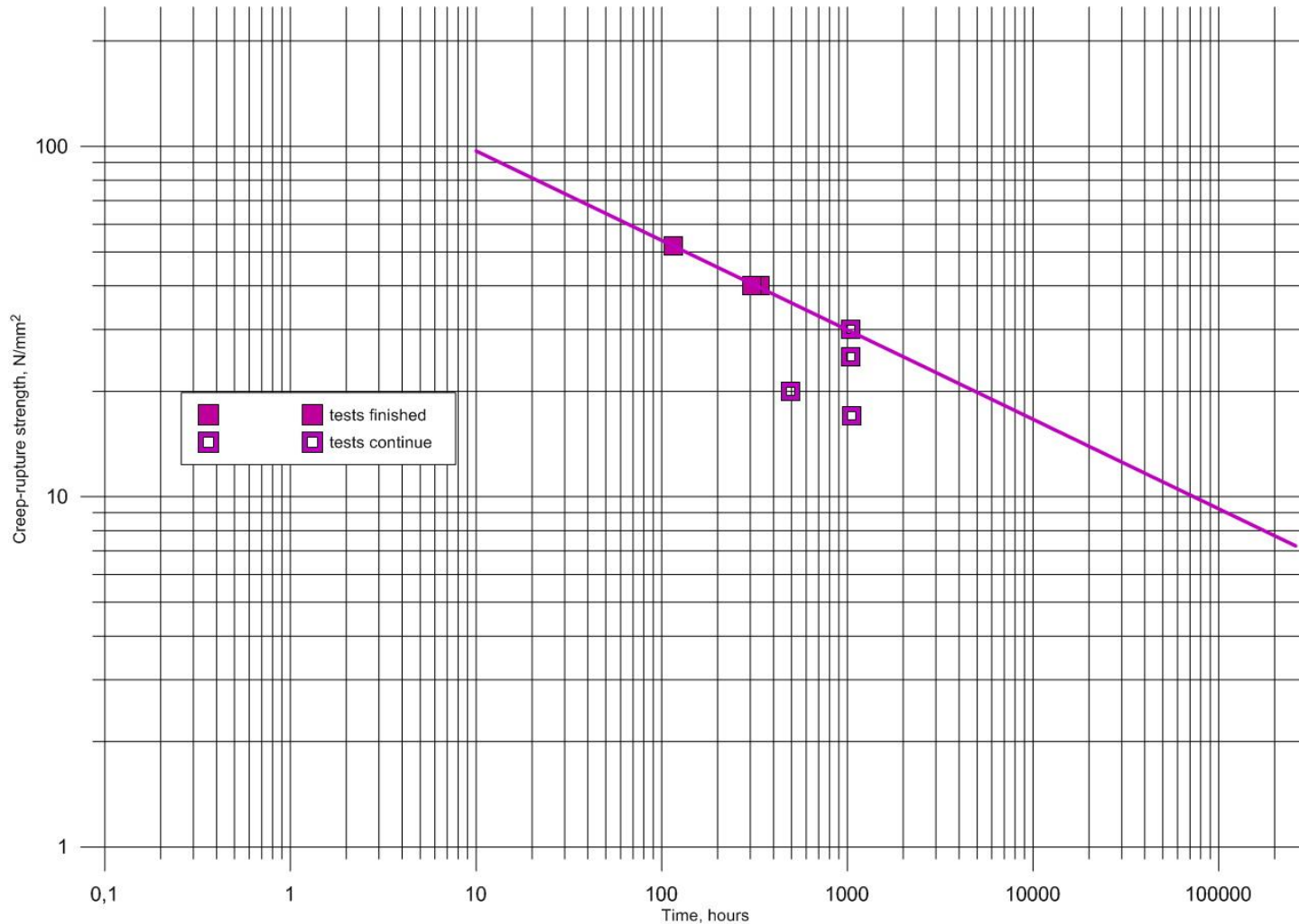
| | Yield strength ($R_{p0,2}$), N/mm ² | Ultimate strength (R_m), N/mm ² | Percentage elongation (A_5),% | Ultimate strength (R_m), N/mm ² |
|--------------|---|--|---|--|
| | Welded metal | | | Wire |
| SV-08Mn2Si-0 | 420-426 | 540-543 | 25-27 | 1000, 1095, 1095 |

| Test temperature, T, °C | Stress, σ , N/mm ² | Time to rupture, τ , hours. | Percentage elongation, A, % | Percentage reduction of area, Z, % | Parameter, P _{CR} |
|----------------------------|--------------------------------------|----------------------------------|-----------------------------|------------------------------------|----------------------------|
| Operating temperature | 50 | 199 | 40,7 | 71,2 | 18,696 |
| | 40 | 547 | 50,2 | 61,2 | 19,081 |
| | 40 | 418 | 61,3 | 68,4 | 18,978 |
| | 30 | 1048 | Tests are continued | | 19,327 |
| | 35 | 500 | | | 19,046 |
| | 35 | 500 | | | 19,046 |
| | 25 | 1044 | | | 19,326 |
| | 20 | 496 | | | 19,045 |
| | 17 | 1051 | | | 19,328 |
| Operating temperature + 50 | 30 | 116 | 77,0 | 82,5 | 19,506 |
| | 30 | 141 | 72,0 | 75,6 | 19,586 |
| | 25 | 241 | 55,7 | 79,6 | 19,799 |
| | 25 | 269 | 72,8 | 82,1 | 19,844 |
| | 17 | 651 | 71,1 | 73,0 | 20,198 |
| | 17 | 797 | 60,3 | 74,7 | 20,279 |
| | 20 | 520 | Tests are continued | | 20,108 |
| | 20 | 520 | | | 20,108 |
| | 13 | 328 | | | 19,923 |

| Test temperature, T, °C | Stress, σ , N/mm ² | Time to rupture, τ , hours. | Percentage elongation, A, % | Percentage reduction of area, Z, % | Parameter P _{CR} |
|---------------------------|--------------------------------------|----------------------------------|-----------------------------|------------------------------------|---------------------------|
| Operating temperature | 52 | 116 | 18,7 | 52,0 | 18,492 |
| | 40 | 339 | 31,6 | 80,4 | 18,899 |
| | 40 | 305 | 13,9 | 34,0 | 18,858 |
| | 30 | 1048 | Tests are continued | | 19,327 |
| | 25 | 1044 | | | 19,326 |
| | 20 | 496 | | | 19,045 |
| | 17 | 1051 | | | 19,328 |
| 13 | 328 | 19,923 | | | |
| Operating temperature +50 | 25 | 126 | 32,6 | 46,0 | 19,541 |
| | 25 | 174 | 19,9 | 34,9 | 19,670 |

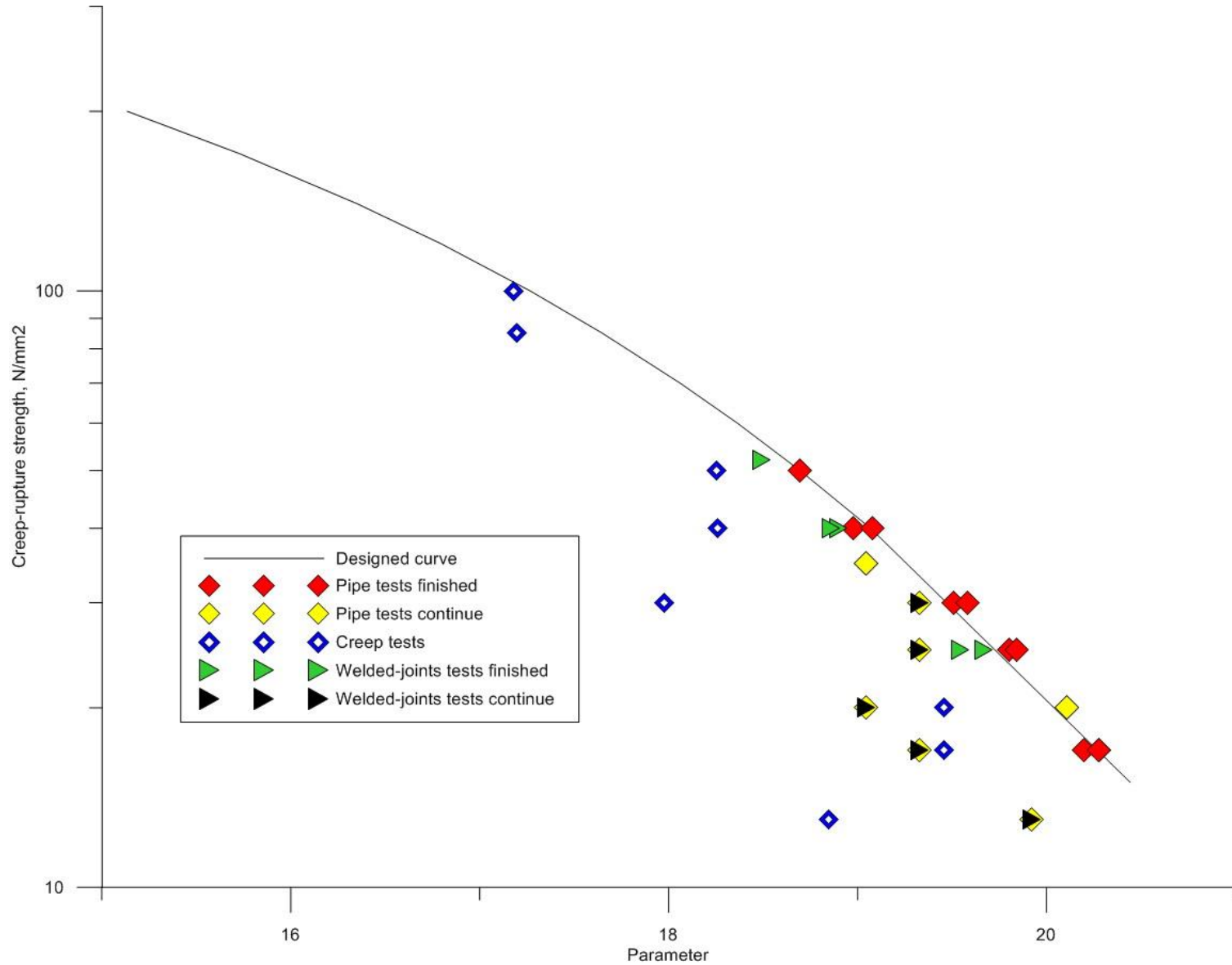




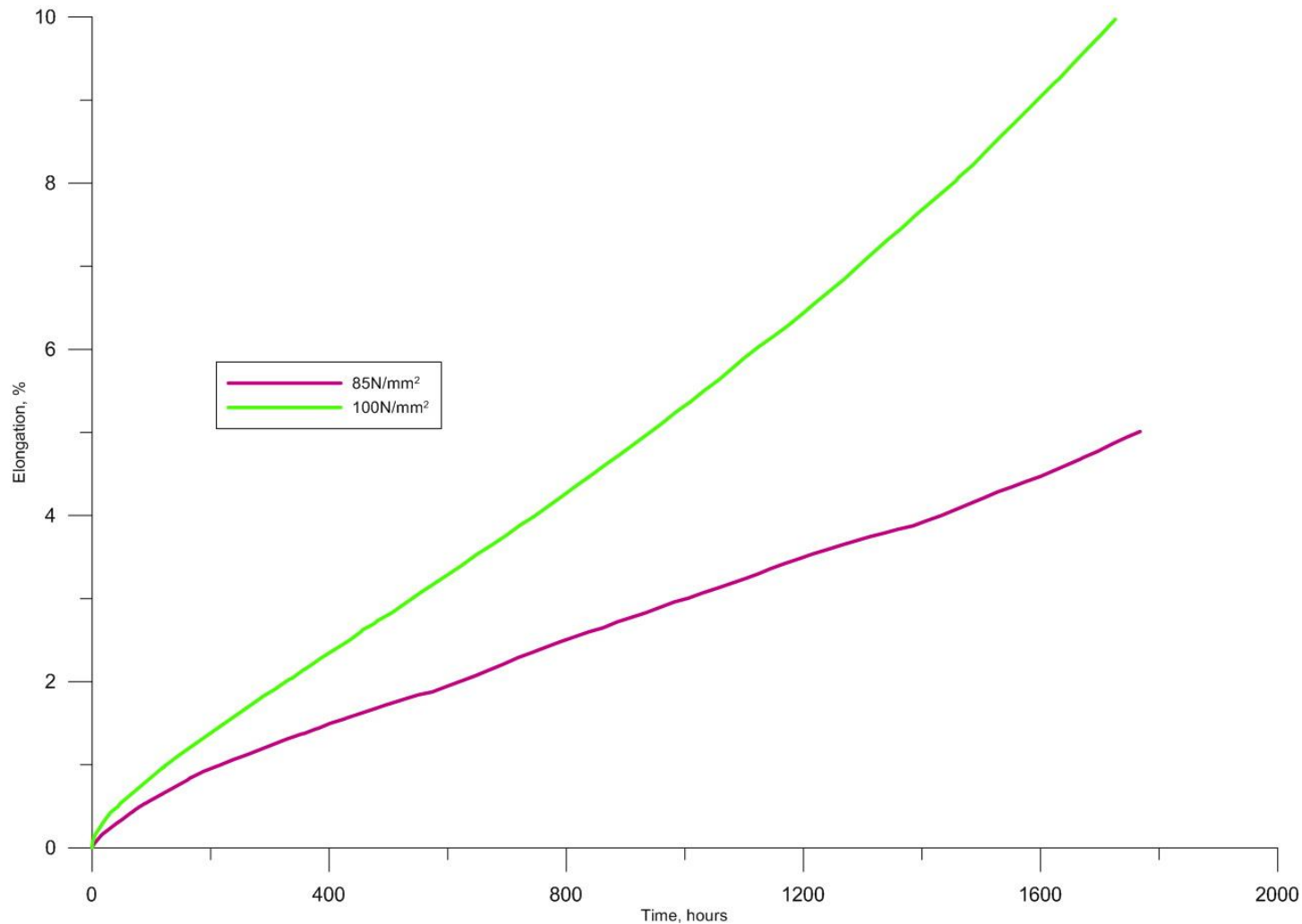


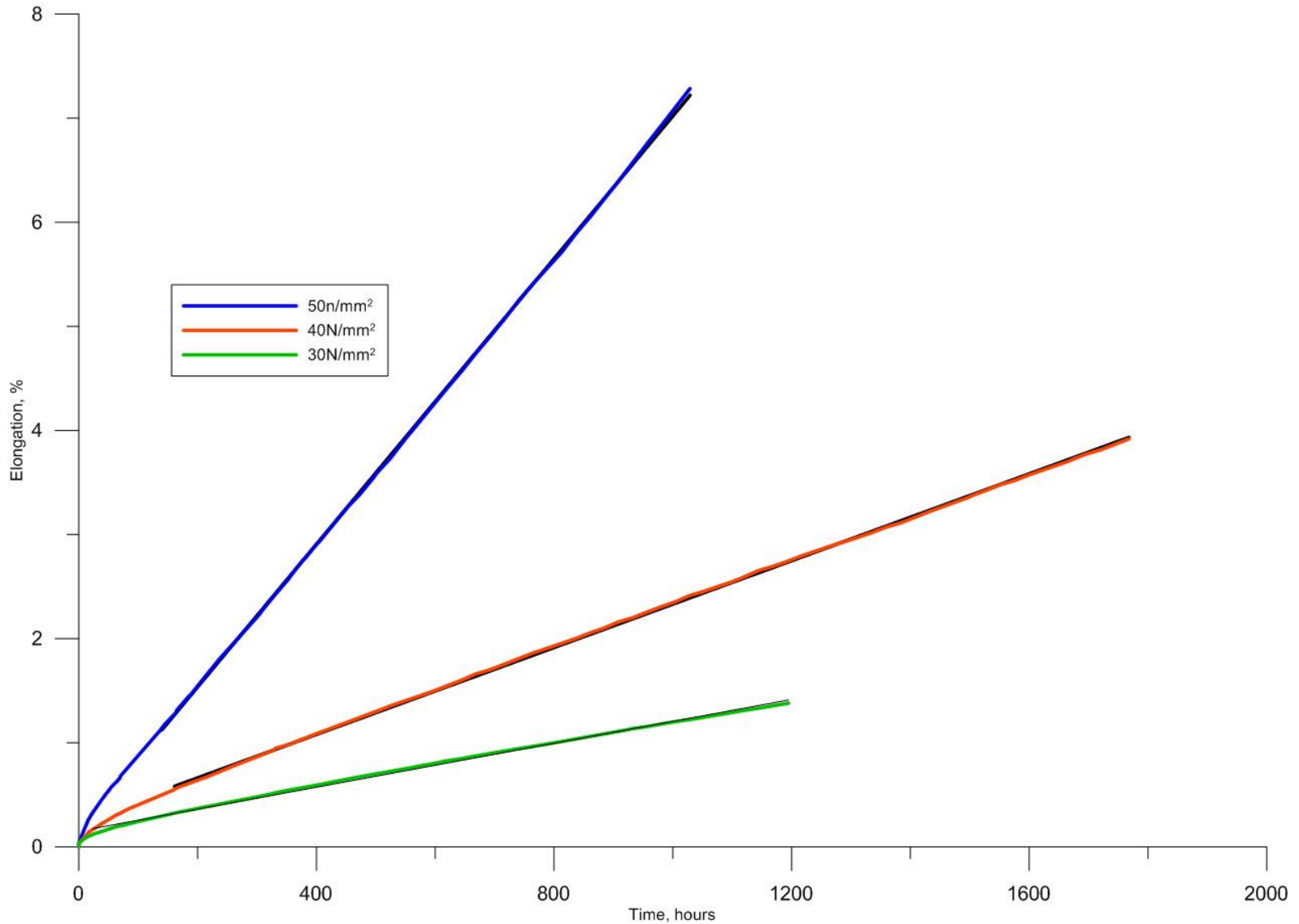
| Temperature | Creep-rupture strength, N/mm ² | | |
|-----------------------------|---|-----------------|---------------------|
| | Lifetime, hours | | |
| | 10 ⁴ | 10 ⁵ | 2,6·10 ⁵ |
| Pipes metal | | | |
| Operating Temperature | 22-23 | 14-15 | 11-12 |
| Operating Temperature+ 50°C | 10 | 6 | 3-4 |
| Welded joint | | | |
| Operating Temperature | 17-18 | 9 | 7 |

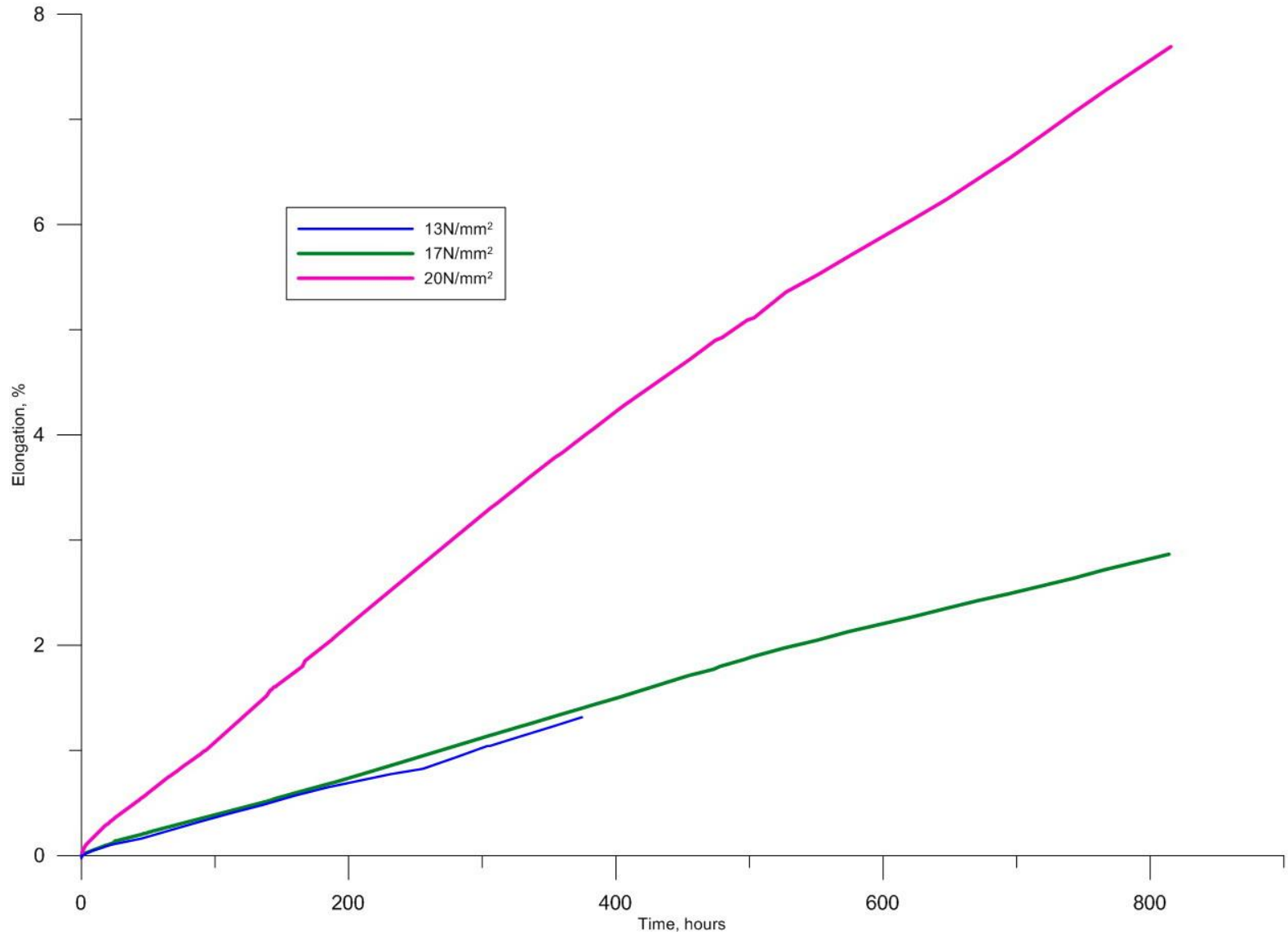




| Test temperature, °C | Stress σ , N/mm ² | Test time τ , hours. | Sample elongation ϵ , % |
|----------------------------|-------------------------------------|---------------------------|----------------------------------|
| Operating Temperature -100 | 100 | 1004 | 5,35 |
| | 85 | 1049 | 3,12 |
| Operating Temperature -50 | 50 | 1024 | 7,29 |
| | 40 | 1047 | 2,45 |
| | 30 | 474 | 0,68 |
| Operating Temperature | 20 | 1027 | 9,55 |
| | 17 | 1025 | 3,55 |
| | 13 | 300 | 0,91 |







- 1 The aim of this development was to obtain the insufficient data necessary to justify service characteristics used in the evaluation of the strength, safety and lifetime of seamless hot-formed pipes of 09Mn2Si steel and their welded joints intended for the construction of structural elements of the reactor vessel heating system BREST-OD-300. And the test program was designed.
- 2 To conduct tests, welded joints are made by the standard technology - using the same technological documents and using the same welding materials as the welded joints of the reactor vessel heating system BREST-OD-300. These welded joints were made by welding materials, made according to the same normative documents, identical to those used for welding joints of the structural elements of the reactor vessel heating system BREST-OD-300
- 3 Creep-rupture strength tests for thick-walled 09Mn2Si pipe samples were carried out at two temperatures: operating temperature, (operating temperature + 50°C). Creep-rupture strength tests for welded joint samples were carried out at operating temperature. Values of creep-rupture strength limits are obtained. On limited test duration, creep-rupture diagrams of 09Mn2Si pipe metal and welded joint for operating temperature and operating temperature + 50°C are constructed.
- 4 The preliminary values of creep-rupture strength (R_{mt}^T) of 09Mn2Si steel and its welded joints, at operating temperature was determined for lifetime 10^4 , 10^5 and $2,6 \times 10^5$ hours. Value of creep-rupture strength (R_{mt}^T) of 09Mn2Si steel at lifetime $2,6 \times 10^5$ hours is 11-12 N/mm². Value of creep-rupture strength (R_{mt}^T) of welded joint at lifetime $2,6 \times 10^5$ hours is around 7 N/mm²
- 5 The percentage elongation of 09Mn2Si pipes at operating temperature, (operating temperature + 50°C is from 40 to 77 percents
- 6 Creep-rupture strength reduction of the welded joint is 25-30% compared to pipe metal.
- 7 The large scale formation of 09Mn2Si pipes was noted for high temperatures
- 8 Primary elongation-time diagram for operating temperature, (operating temperature - 50 ° C) and (operating temperature - 100 ° C) are constructed.
- 9 Considering the large scale formation, obtained values for creep-rupture strength limits are approximate. And based on obtained values, critical temperature of 09Mn2Si steel pipes can be determined
- 10 Based on the results of the development, it is possible to draw conclusions about continuation of research to justify the strength, safety and lifetime of structural elements material of the reactor vessel heating system BREST-OD-300.

THANK YOU FOR ATTENTION!

CONTACTS:

Head of laboratory
JSC RPA «CNIITMASH»

Sergey Logashov
SULogashov@cniitmash.com

+7 (495) 675-85-42;

+7 (926) 176-79-50



РОСАТОМ

**JSC «D.V. Efremov Institute of
Electrophysical Apparatus»**



ПРЕДПРИЯТИЕ ГОСУДАРСТВЕННОЙ КОРПОРАЦИИ ПО АТОМНОЙ ЭНЕРГИИ «РОСАТОМ»

Facility GESA-4M for electron beam modification of fuel cladding surfaces of reactor plants with heavy liquid metal coolant

Engelko V.I., Pavlov E.P., Tkachenko K.I., Shchegolikhin N.P.

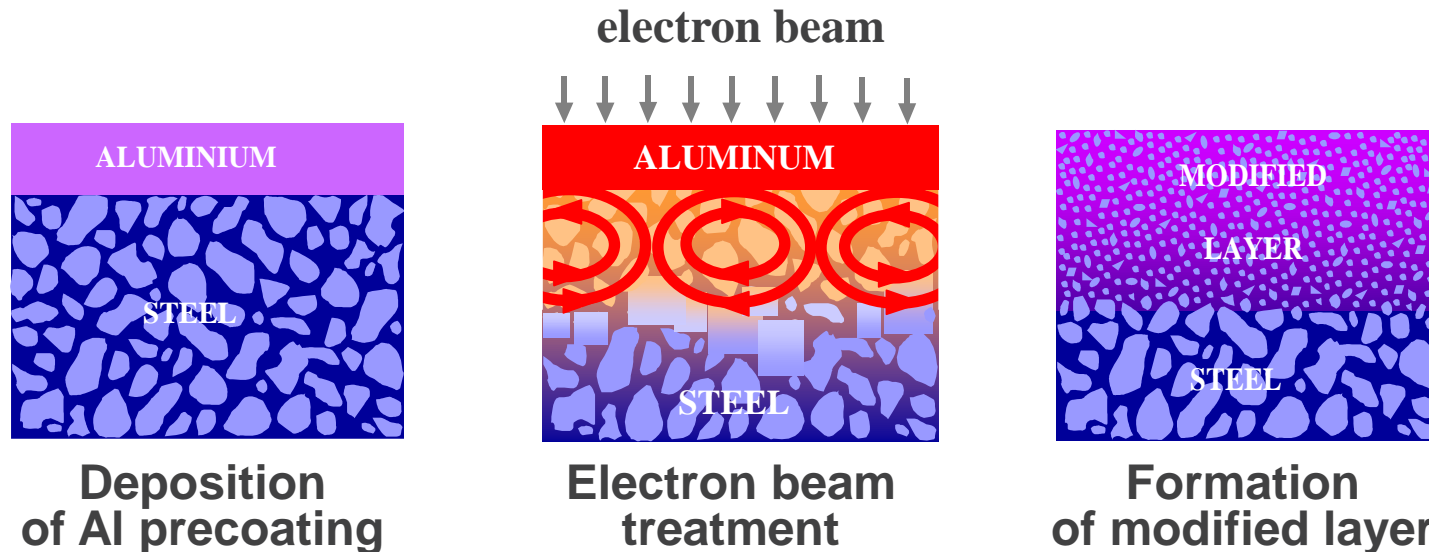
**Obninsk
HLMC-2018**

08-10.10.2018



Formation of AL enriched surface layers with the help of MIEB

For improvement of the corrosion resistance of structural steels operating in Pb and Pb-Bi coolant it was suggested to modify material surface properties by Al with the help of high-current pulse electron beams - HPEB-SM process, or GESA process





The process (so-called GESA process) was studied by

- D.V. Efremov Institute of Electrophysical Apparatus, Russia;
- A.I. Leypunsky Institute of Physics and Power Engineering, Russia;
- Central Research Institute of Structural Materials PROMETHEY, Russia;
- Karlsruhe Institute of Technology (FZK), Germany.

The objective

- **Corrosion resistance in Pb and Pb-Bi up to 650 °C.**
- **No negative influence on mechanical properties.**
- **Self healing of mechanically damaged layers.**
- **The modification process must be of industrial relevance.**

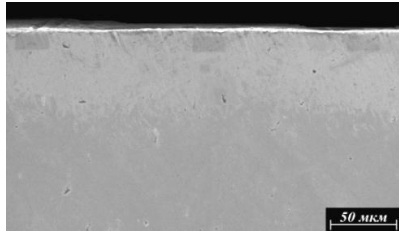


Optimal procedure of GESA + Al modification of steel surface:

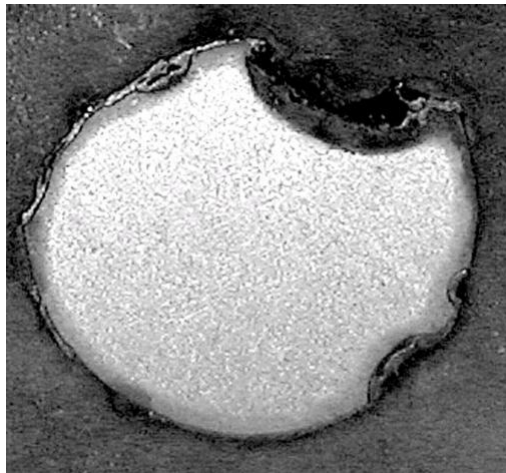
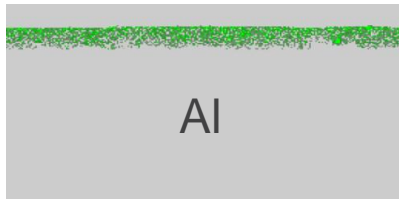
- **electropolishing of austenitic steels surface and mechanical polishing of ferrite-martensitic steels surface before precoating deposition,**
- **ultrasonic cleaning and ion beam etching of the steel surface,**
- **precoating thickness 5-7 μm ,**
- **heating of specimens with precoating before MIEB treatment at 200°C during 2 hours,**
- **energy density of electron beam at the surface 40-45 J/cm^2 ,**
- **number of electron beam pulses – 2-3.**



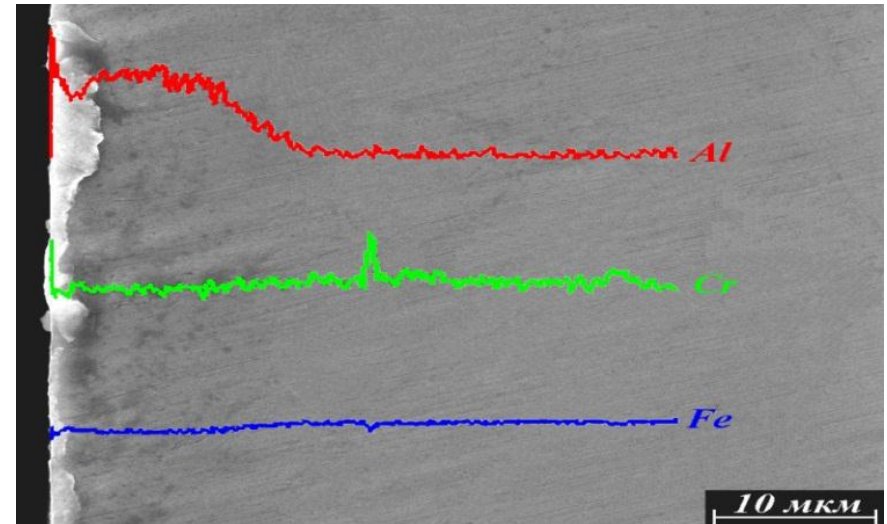
STC «Laser complexes and technologies»



Modified layer of T91 steel specimen (5 μm Al + GESA) after corrosion test in Pb-Bi flow in the loop CU-2M at $T=550^{\circ}\text{C}$ for 16547 hours and $C_{[\text{O}]} = (1-4) \cdot 10^{-6}$ wt. %.



T91 steel in original state after corrosion test in Pb-Bi flow in the loop CU-2M at $T=550^{\circ}\text{C}$ for 16547 hours and $C_{[\text{O}]} = (1-4) \cdot 10^{-6}$ wt. % (the stem of the specimen)



— Al
— Cr
— Fe

Distribution of the elements in a surface layer of the modified T91 steel specimen (5 μm Al + GESA) after corrosion test in Pb-Bi flow in the loop CU-2M at $T=550^{\circ}\text{C}$ for 16547 hours and $C_{[\text{O}]} = (1-4) \cdot 10^{-6}$ wt. %



EP823 steel surface modification by pulsed electron beams

Tests parameters: Pb flow, $T=650^{\circ}\text{C}$, $v=1,5\text{ m/s}$, $C_{[\text{O}]}=(5-8)\cdot 10^{-5}\text{ wt \%}$

Not modified
Oxygen corrosion



1000 h

Modified
No corrosion



3000 h



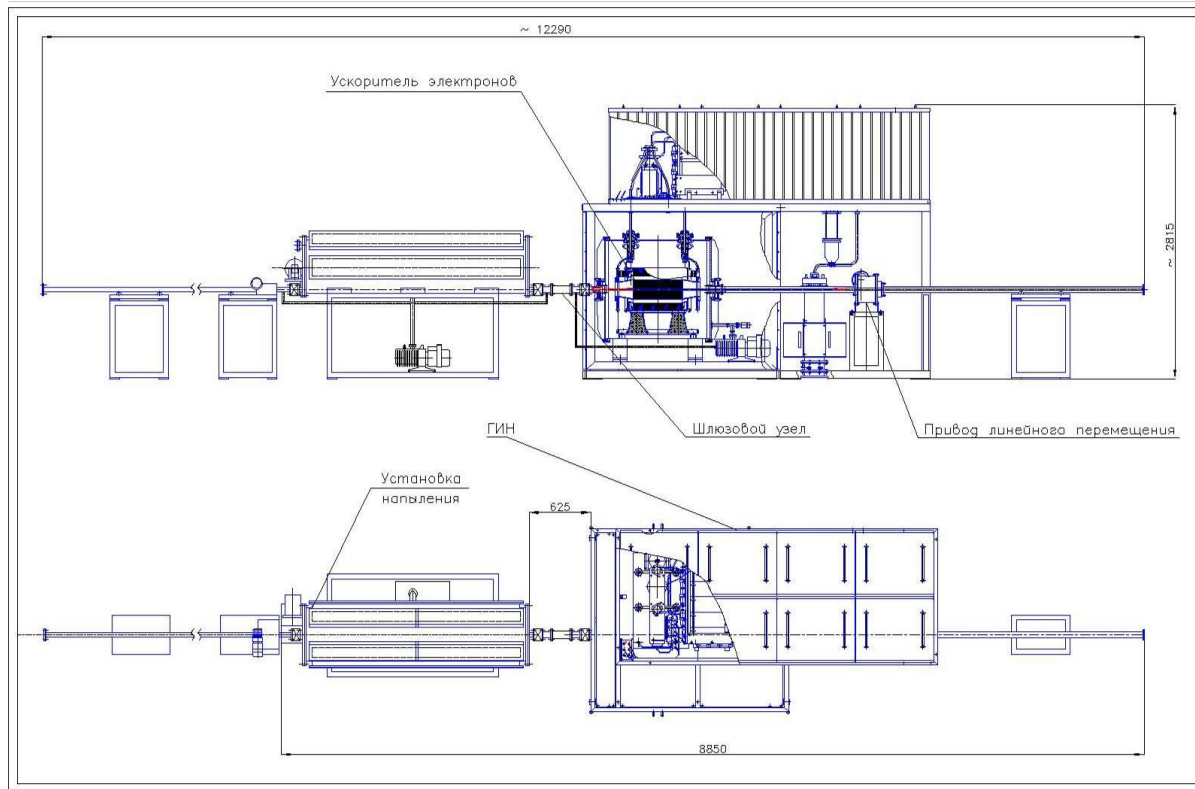
5000 h



Technical requirements to industrial facility

Cladding parameters:

pipes made from EP823 steel $\text{Ø}10.5$ (9.7) мм, wall thickness 0,5 мм, total length 2140 мм, length in contact with Pb 1100 мм.





Main technical parameters of the sputtering facility:

- number of magnetrons 4-6;
- coated area – diameter 10.5 (9.7) mm, length up to 2140 mm;
- number of simultaneously coated claddings 25;
- duration of fabrication cycle (loading-pumping-coating-unloading) for coating thickness 5 MKM 60 min;
- power consumption 210 kW.

Main technical parameters of the electron beam facility:

- electron energy up to 120 keV;
- beam energy density on the target 40 – 45 J/cm²
- pulse duration 30 – 80 μs;
- beam length 70 - 80 cm;
- repetition rate 0,033 1/s
- power consumption 20 kW



Components of the surface modification module of claddings



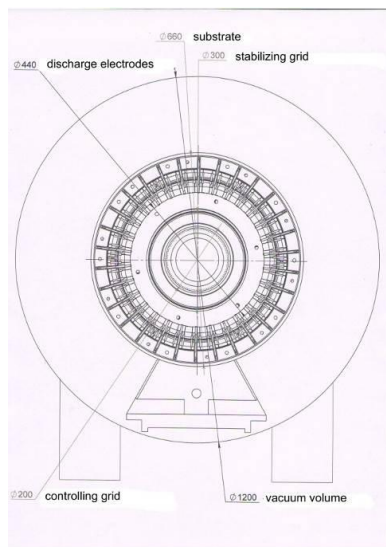
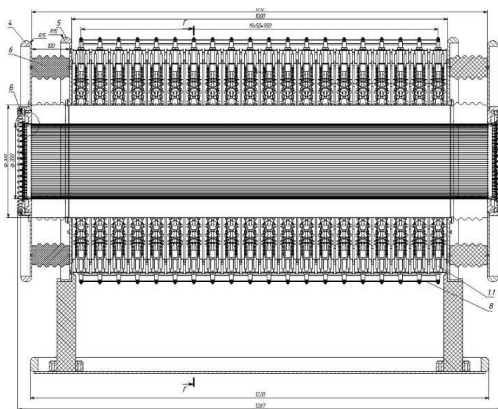
Electron beam facility



Precoating deposition facility



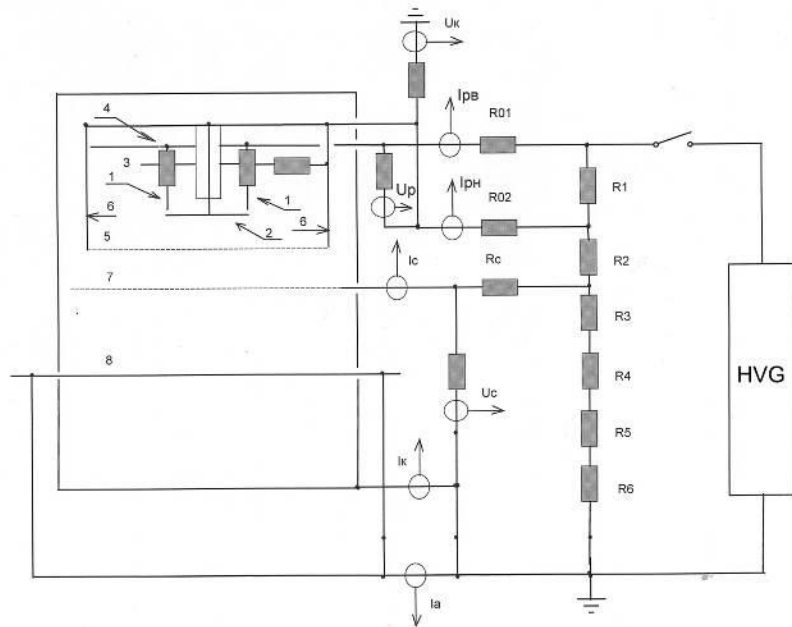
Parameters of electron source



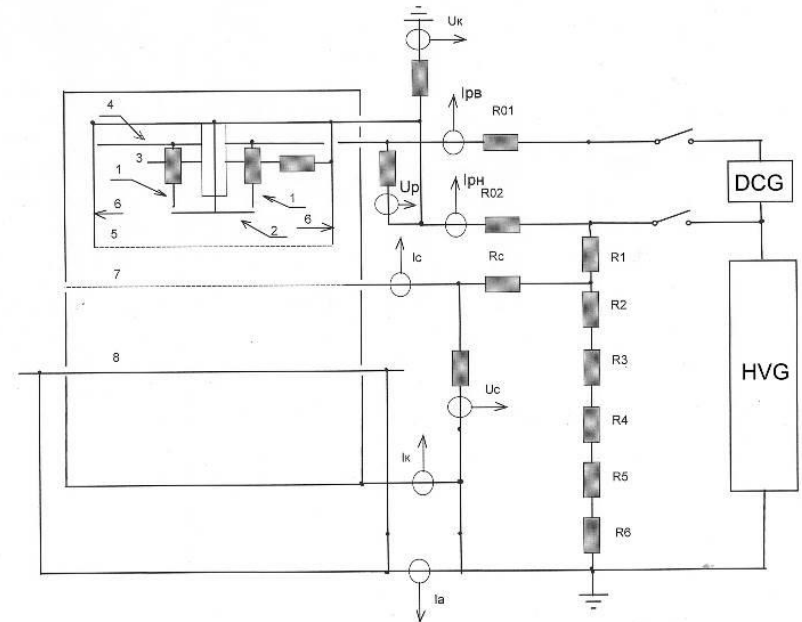
| | |
|------------------------|-----------------------|
| Voltage of anode, kV | $U_A = 0$ |
| Voltage of cathode, kV | $U_C = -120$ |
| Voltage of grid, kV | $U_g = -(97 \div 95)$ |
| Radius of cathode, m | $R_C = 0,15$ |
| Radius of grid, m | $R_g = 0.1$ |
| Radius of anode, m | $R_A = 0.005$ |
| Length of anode, m | $L_C = 0,95$ |



Electrical schemes of supply for source electrodes



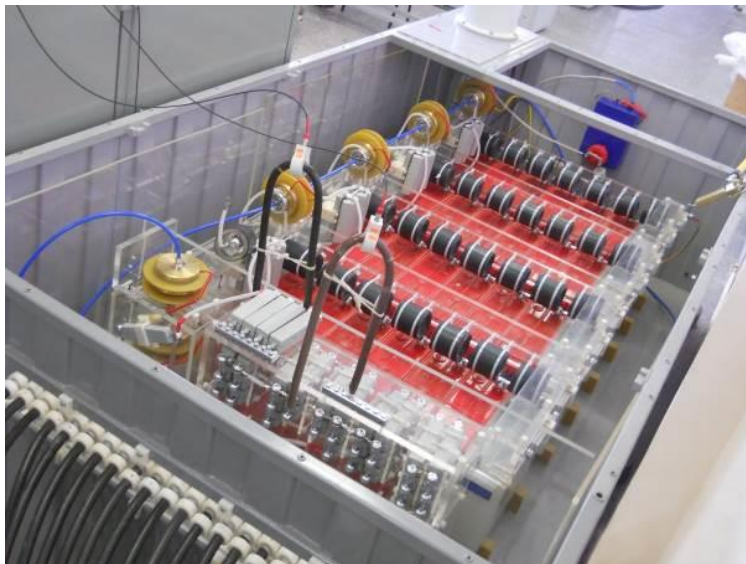
Potentials of cathode, discharge gaps and control grid are determined by divider R_1 - R_6 , which is connected to output of pulse high voltage generator (HVG)



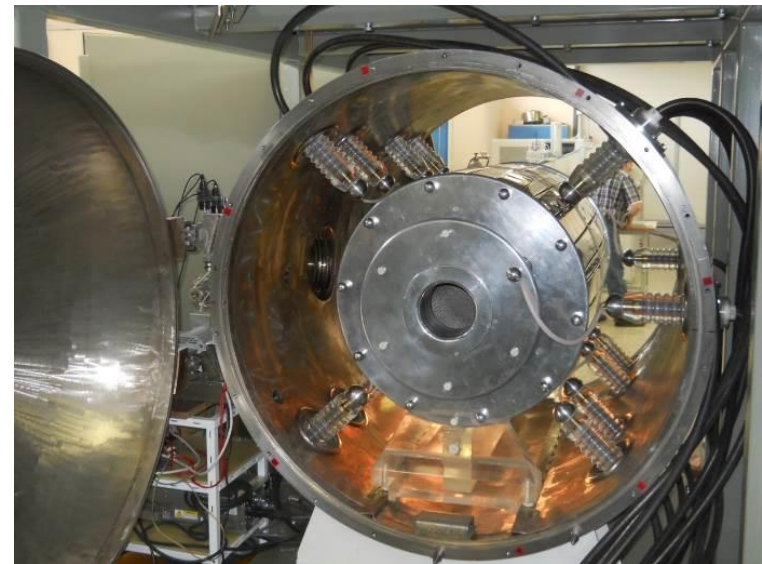
It is used 5-stage HVG . The stage connected to discharge gaps has autonomic charging circuit, that allows to regulate amplitude of discharge current independently on accelerating voltage



Components of the electron beam facility



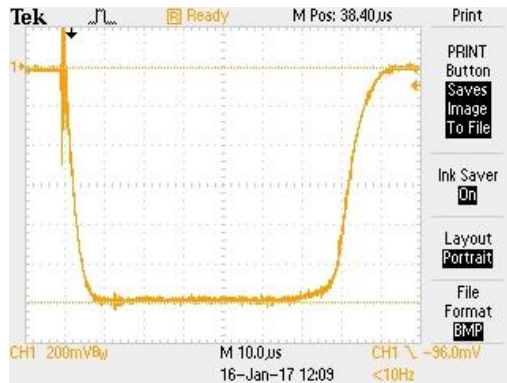
Overview of HVG



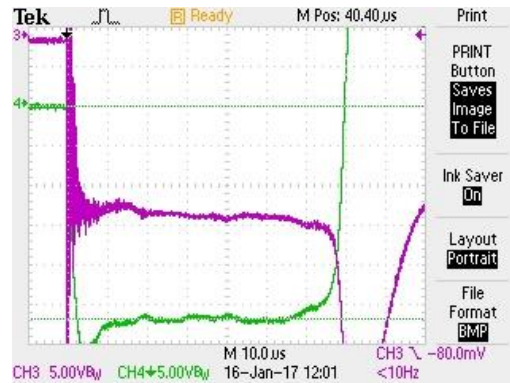
Overview of the electron source



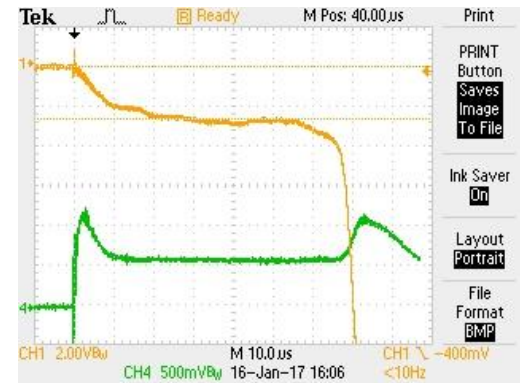
Typical oscillograms of pulse electron beam



a



b



c

a - accelerating voltage U_k

b - discharge currents I_{pB} и I_{pH}

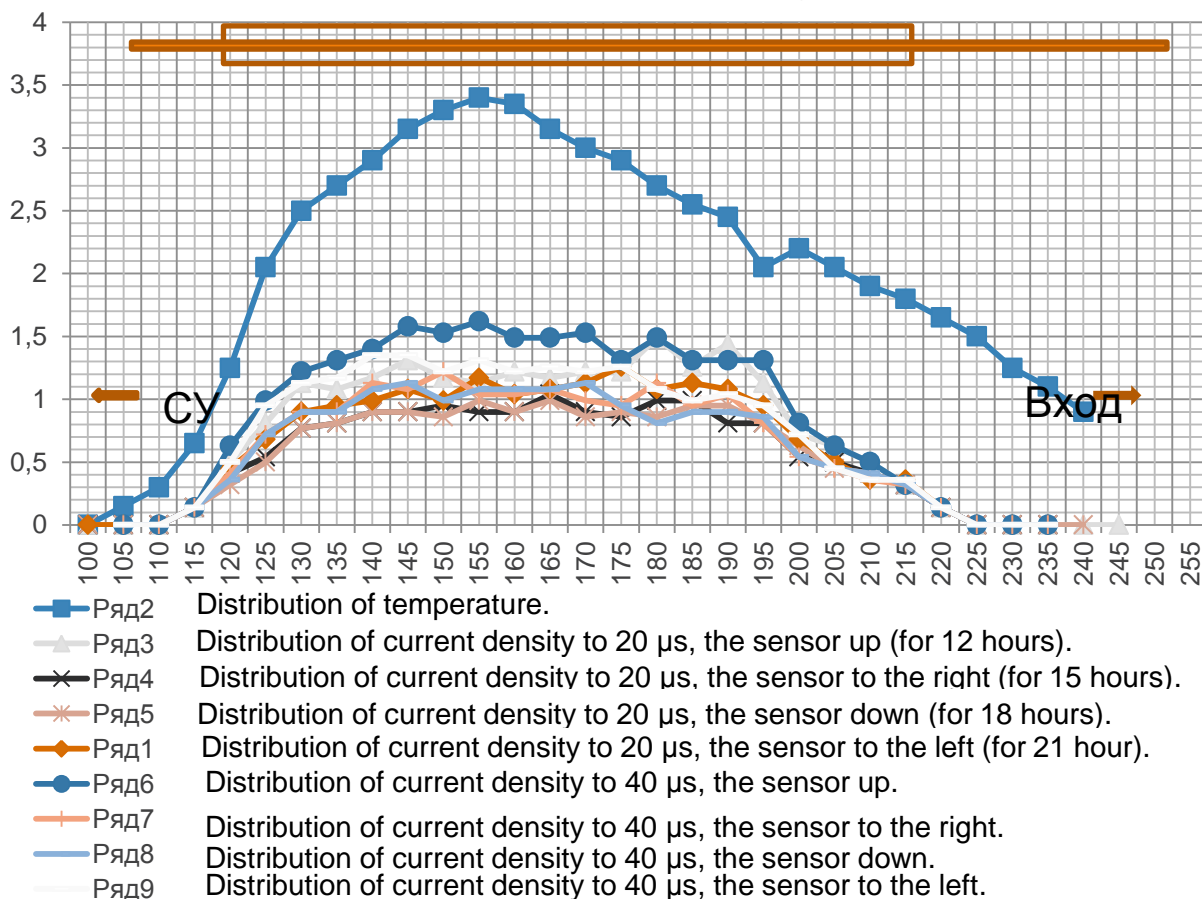
c – anode current (current on target) I_a

voltage between base plate and setting fire electrodes U_p



STC «Laser complexes and technologies»

Distribution of current density on Ø10 mm target on the GESA-4M facility



Typical view of distribution of temperature and anode current density on 1-meter target



Conclusions

1. Maximal value of energy density of electron beam achieved on the target with diameter 10 mm was 30 J/cm^2 for central part of target ~ 50 cm.
2. For increasing of beam current and accordingly of energy density of electron beam it is supposed:
 - to isolate stabilizing grid from cathode assembly and to optimize its potential ;
 - to set in front of target distantly 1,5 cm from axis additional grid with high transparency to eliminate virtual cathode.

Контактная информация

Ткаченко Константин Иванович,
Head of group, PhD (Tech.)

RD LK-2 RL KL-5

+7 (812) 464-5864

ktkachenko@mit.niiefa.spb.su

www.niiefa.spb.su

